Bcl6 and Blimp1 reciprocally regulate ST2^{+} Treg cell development in the context of allergic airway inflammation

Byunghee Koh, PhD [1,2], Benjamin J. Ulrich, PhD [2], Andrew S. Nelson, PhD [1], Gayathri Panangipalli, BS [3], Rakshin Kharwadkar, MS [4], Wenting Wu, PhD [5], Markus M. Xie, PhD [2], Yongyao Fu MS [2], Matthew J. Turner, MD, PhD , Sophie Paczesny, MD, PhD [1,2], Sarath Chandra Janga, PhD [3], Alexander L. Dent, PhD [2], and Mark H. Kaplan, PhD [1,2]

[1]Department of Pediatrics and Herman B Wells Center for Pediatric Research
Indiana University School of Medicine, Indianapolis, IN 46202

[2] Department of Microbiology and Immunology, Indiana University School of Medicine, Indianapolis, IN, 46202

[3] Department of Biohealth Informatics, School of Informatics and Computing, Indiana University-Purdue University, Indianapolis, IN 46202

[4] Department of Biochemistry and Molecular Biology, Indiana University School of Medicine, Indianapolis, IN, 46202

[5] Department of Medical and Molecular Genetics, Indiana University School of Medicine, Indianapolis, IN, 46202

[6] Department of Dermatology, Richard L. Roudebush VA Medical Center, Indianapolis, IN 46202

Corresponding author
Mark H Kaplan, PhD

This is the author's manuscript of the article published in final edited form as:

Koh, B., Ulrich, B. J., Nelson, A. S., Panangipalli, G., Kharwadkar, R., Wu, W., ... & Janga, S. C. (2020). Bcl6 and Blimp1 reciprocally regulate ST2+ Treg cell development in the context of allergic airway inflammation. Journal of Allergy and Clinical Immunology. https://doi.org/10.1016/j.jaci.2020.03.002

Indiana University School of Medicine
Department of Microbiology and Immunology
635 Barnhill Dr. Room 420
Indianapolis, IN 46202
United States of America
Ph: +1-317-278-3696
Email: mkaplan2@iu.edu

Funding: This work was supported by PHS grants from the National Institutes of Health R01 AI057459 to M.H.K. and R01 AI132771 to A.L.D. BJU was supported by T32 AI060519 and F30 HL147515. ASN was supported by T32 HL007910. M.M.X. was supported by a Careers in Immunology Fellowship from American Association of Immunologists. MJT was supported by the Department of Veterans Affairs grant IK2 CX001019 (VA CDA2). Core facility usage was also supported by IU Simon Cancer Center Support Grant P30 CA082709 and U54 DK106846. Support provided by the Herman B Wells Center was in part from the Riley Children's Foundation.

Conflicts of Interest: The authors declare no conflicts of interest.

Abstract

Background: Bcl6 is required for the development of T follicular helper and regulatory (Tfh, Tfr) cells that regulate germinal center responses. Bcl6 also impacts the function of regulatory T (Treg) cells.

Objective: The goal of this study is to define the functions of Bcl6 in Treg cells including Tfr cells in the context of allergic airway inflammation (AAI).

Methods: We employed a model of house dust mite (HDM) sensitization to challenge wild type, *Bcl6*$^{fl/fl}$ Foxp3-Cre and *Prdm1*(Blimp1)$^{fl/fl}$ Foxp3-Cre mice to study the reciprocal roles of Bcl6 and Blimp1 in AAI.

Results: In the HDM model, Tfr cells repress the production of IgE and Bcl6+ Treg cells suppress the generation of type 2 cytokine producing cells in the lungs. In mice with Bcl6-deficient Treg cells, twice as many ST2 (IL-33R)$^{+}$ Tregs develop as observed in wild type mice. ST2^{+} Tregs in the context of AAI are Blimp1-dependent, express type 2 cytokines, and share features of visceral adipose tissue Treg cells. Bcl6-deficient Tregs are more susceptible, and Blimp1-deficient Tregs are resistant, to acquiring the ST2^{+} Treg cell phenotype in vitro and in vivo in response to IL-33. Bcl6-deficient ST2+ Tregs but not Bcl6-deficient ST2+ T conventional cells strongly promote AAI when transferred into recipient mice. Lastly, ST2 is required for the exacerbated AAI in *Bcl6*$^{fl/fl}$ Foxp3-Cre mice.

Conclusions: During AAI, Bcl6 and Blimp1 play dual roles in regulating Tfr activity in the germinal center and in the development of ST2^{+} Tregs that promote type 2 cytokine responses.

Key Messages:

- Tfr cells limit IgE production in mice challenged by airway allergen
- Bcl6 and Blimp1 reciprocally regulate $ST2^+$ Treg development
- $ST2^+$ Tregs promote allergic airway inflammation

Capsule Summary: Bcl6 attenuates allergic disease by promoting Tfr cell development to repress the allergen-specific humoral response and by limiting expansion of $ST2^+$ Tregs.

Keywords: interleukin-33, ST2, Bcl6, Blimp1, T follicular regulatory T cells, ST2-expressing regulatory T cells, allergy, asthma.

Abbreviations:

AAI: Allergic airway inflammation

BAL: Bronchoalveolar lavage

ChIP: Chromatin Immunoprecipitation

ELISA: Enzyme-linked immunosorbent assay

Foxp3: Forkhead box P3

GC: Germinal center

HDM: House dust mite

iTreg: in vitro cultured Treg

mLN: mediastinal lymph node

mesLN: mesenteric lymph node

PMA: Phorbol 12-myristate 13-acetate

Prdm1: gene encoding Blimp1

pTreg: Peripheral regulatory T cell

Tconv: Conventional T cell

Tfh: T follicular helper cell

Tfr cells: T follicular regulatory T cells

Treg: Regulatory T

VAT: visceral adipose tissue

WT: Wild-type

Introduction

Bcl6 is a transcriptional repressor that is a central regulator of immunity with functions in T cells, macrophages and B cells (1-7). Bcl6 is critical for the germinal center response, controlling both T follicular helper (Tfh) cells and Germinal Center B (GC) B cells (1-6). Bcl6 is also expressed in a population of cells co-expressing Foxp3, the lineage defining factor for regulatory T (Treg) cells. Like Tfh and GC B cells, these cells termed T follicular regulatory (Tfr) cells co-localize to the germinal center (8-10).

In the GC, Tfh cells help B cells to produce high affinity antigen specific antibodies (Abs) (11, 12). However, dysregulated Tfh cells promote B cells production of self-reactive Abs leading to autoimmune disease (13-15). It was proposed that Tfr cells regulate excessive GC reactions by suppressing proliferation of Tfh and self-reactive B cells (8-10, 16, 17). However, recent studies report that Tfr cell-derived IL-10 is important for maintenance of the GC response and provides helper functions for the antibody response (18). Thus, the regulatory and helper functions of Tfr cells might differ depending on the context of the immune response.

In the context of allergic disease, characterized by production of Th2 cytokines such as IL-4, IL-5 and IL13, and allergen specific IgE, Bcl6 likely has multiple functions. Previous reports have shown increased allergic inflammation in mice that have germline deletion of Bcl6 (19-22). Enhanced allergic inflammation was thought, at least in part, to be from effects of Bcl6-deficiency in Treg populations that resulted in increased Th2 cytokines and expression of genes including *Il1rl1*, which encodes the IL-33R, ST2 (22). In the absence of Tfh cells, using mice that lack Bcl6 in all $CD4^+$ T cells, there is no IgE production in response to allergen sensitization and the absence of IgE-dependent immune function (23). In allergic pulmonary inflammation it is unclear how Bcl6 influences Treg function.

In this study, we revealed that Tfr cells are critical for the allergen-specific humoral immune response during HDM induced airway inflammation. Tfr cell deficiency increased total and antigen specific IgE production and Th2 responses contributing to more severe airway inflammation. The development of $ST2^+$ Treg cells was reciprocally regulated by Bcl6 and Blimp1. Bcl6-deficiency promoted $ST2^+$ Treg cell development in mediastinal lymph node (mLN) and lung, and the increased pulmonary inflammation was ST2-dependent, defining a critical role for Bcl6 in restraining the development of pro-allergic $ST2^+$ Treg cells.

METHODS

Mice

All mice were C57BL/6 background, except as specified for BALB/cJ mice in strain comparisons. BALB/cJ, C57BL/6, *Foxp3*-Cre^{YFP}, *Bcl6*$^{fl/fl}$Foxp3-Cre^{YFP}, *Bcl6*$^{fl/fl}$CD4-Cre^{YFP}, *Prdm1*$^{fl/fl}$Foxp3-Cre^{YFP}, *Il1rl1*$^{-/-}$, *Il1rl1*$^{-/-}$*Bcl6*$^{fl/fl}$Foxp3-Cre^{YFP} were maintained under specific pathogen-free conditions. C57BL/6 x B6.SJL-Ptprc^{a}Pepc^{b}/BoyJ F1 mice were used as recipients for adoptive transfer experiments. All experiments were done with 6–8 week-old mice. All experiments were performed with the approval of the Indiana University Institutional Animal Care and Use Committee.

Treg cell culture

Naïve CD4^{+}CD62L^{+} T cells from mice were positively selected from the enriched CD4^{+} T cells from spleen and lymph nodes using MACS beads and columns (Miltenyi Biotec). Naive CD4^{+}CD62L^{+} T cells were activated with plate-bound anti-CD3 (2 μg/ml 145-2C11 ; BioXCell) and soluble anti-CD28 (0.5 μg/ml ; BD Pharmingen) in complete culture media, Roswell Park Memorial Institute 1640 (RPMI 1640, ThermoFisher Scientific) containing 10% Fetal bovine serum (FBS, Atlanta Biologicals), 1% antibiotics (penicillin and streptomycin / stock; Pen 5000 μ/ml, Strep 5000 μg/ml), 1 mM sodium pyruvate, 1 mM L-Glutamine, 2.5 ml of Non-essential amino acids (Stock; 100 X), 5mM HEPES (all from LONZA) and 57.2 μM 2-Mercapoethanol (Sigma-Aldrich), to generate Treg cells (5 ng/ml hTGF-β1, 10U/ml hIL-2, 10 μg/ml anti-IFNγ,10 μg/ml anti-IL-4 or IL-33 1-10ng/ml). For splenic Treg cell culture, YFP^{+} Treg cells were sorted from spleen of *Foxp3*-Cre^{YFP} mice and activated with plate-bound anti-CD3 (2 μg/ml) and

soluble anti-CD28 (0.5 μg/ml), hIL-2 (200U/ml) with IL-33 (1 or 10 ng/ml) in complete culture media. Cells were grown at 37°C under 5% CO_2 and harvested on day 3 for analysis.

House dust mite extract-induced allergic airway inflammation

Mice were challenged intranasally with House dust mite (HDM; Greer Laboratories) extract every other day for 16 days. HDM (25 μg) extract was diluted with PBS (25 μl) and administered into the nose. Mice were sacrificed 1 day after final intranasal challenge. Bronchoalveolar lavage (BAL) cells were collected twice by lavaging the lungs with 1 ml PBS. To prepare single cell suspension from lungs, lung tissues were chopped and incubated with 0.5 mg/ml of collagenase A (Roche) in DMEM at 37°C for 45 mins. After grinding tissues with mesh stainless steel strainer, red blood cells were removed by Ammonium-Chloride-Potassium lysing buffer (LONZA). After stopping the reaction by adding buffer (PBS with 0.5 % BSA), cells were washed with the buffer followed by filtering through 70 μm nylon mesh to remove debris. Single cell suspensions were used for flow cytometry, RNA isolation or CD4 T cell enrichment. For adoptive transfer experiment, $ST2^+$ Treg ($CD4^+$ $ST2^+$ $Foxp3/YFP^+$) or Tconv ($CD4^+$ $ST2^+$ $Foxp3/YFP^-$) cells were sorted from lungs of $CD45.2^+$ *Foxp3*-Cre^{YFP}, *Bcl6*$^{fl/fl}$Foxp3-Cre^{YFP} mice (CD45.2) and 50,000 cells were transferred to naïve F1 (CD45.1) recipient mice via tail injection. Following adoptive transfer, recipient mice were challenged with HDM three times at 1 hour, 24 hours, and 48 hours post adoptive transfer. Mice were sacrificed 1 day after final intranasal challenge.

Reverse transcription (RT) and quantitative real-time PCR (qPCR)_qRT-PCR

Total RNA was extracted using TRIzol reagent (ThermoFisher Scientific) and reverse transcribed using qScript cDNA synthesis kit (Quantabio). For qPCR, Taqman real time PCR assay (ThermoFisher Scientific) was used for gene expression analysis. Gene expression was normalized to housekeeping gene expression (β2-microglobulin). The relative gene expression was calculated by the change-in-threshold $2^{-\Delta CT}$ method. All experiments were performed in duplicate in two independent experiments and results are presented as standard error of means (SEM) of biological replicates. Taqman probes sequences are listed in Table E1.

Flow cytometric analysis

For cytokine staining, lung or BAL cells were stimulated with Phorbol 12-myristate 13-acetate (PMA) (Sigma-Aldrich) and ionomycin (EMD Millipore) for 2 hours followed by monensin (BioLegend) for a total of 6 hours. After fixation with 1% formaldehyde for 10 mins at room temperature, cells were washed two times with FACS buffer (PBS with 0.5 % BSA). For transcription factor staining, cells were fixed with Foxp3/Transcription factor fixation buffer (eBioscience) at 4°C in dark for 30 mins or overnight. For cytokine staining and transcription factor combination staining, cells were fixed with 3.7% formaldehyde for 5 mins at 4°C followed by fixation with Foxp3/Transcription factor fixation buffer at 4°C for 3 hours. Fixed cells were permeabilized with permeabilization buffer (eBioscience) and stained for cytokines and transcription factors with fluorochrome conjugated antibodies at 4°C in dark for one hour. Stained cells were washed two times with FACS buffer and resuspended in FACS buffer for flow analysis. Fluorescent antibodies for flow cytometric analysis are listed in Table E2.

ELISA

IgE capturing antibody (BD bioscience; 553413) was coated on 96 well plate (NUNC) with coating buffer (dH_2O with 0.1 M $NaHCO_3$ pH 9) and incubated at 4°C overnight. After washing the plate three times with wash buffer (PBS with 0.05% Tween-20), ELISA buffer (PBS with 2% BSA) was added to well and incubated at room temperature for one hour. After washing the plate three times with wash buffer, 10-100-fold diluted samples and standard IgE were added and incubated at 4°C overnight. The next day, after washing the plate three times with wash buffer, the biotinylated secondary antibody (BioLegend; 406904) was added and incubated at room temperature for one hour. After washing the plate three times with wash buffer, wash buffer with 0.05% of avidin-alkaline phosphatase (Sigma-Aldrich) was added and incubated at room temperature for one hour. After washing the plate three times with wash buffer, substrate buffer with p-Nitrophenyl Phosphate (PNPP) (Sigma-Aldrich) was added to each well. Reaction was stopped by adding stop solution (1N NaOH) and measured with the Biorad Microplate 680 ELISA reader. For HDM specific IgE and IgG1, ELISA kits (Chondrex) were used.

Chromatin Immunoprecipitation (ChIP)

Splenic Treg cells (1×10^6) were stimulated for three days before being cross-linked for 15 mins with 1% formaldehyde at room temperature with rotation. The reaction was quenched by adding 0.125 M glycine and incubated at room temperature for 5 mins. Cells were washed with ice cold PBS two times. Fixed cells were lysed in cell lysis buffer on ice for 10 mins. Chromosomal DNA was fragmented to a size range of 200-500 bp by ultrasonic processor (Vibra-cell) (30 % amplitude for 8 sets of 10 second bursts). After sonication, debris were removed by centrifugation at 13000 rpm for 10 mins at 4°C and supernatant was transferred to new tube and diluted 10-fold with ChIP dilution buffer. After pre-clearing, the supernatant was incubated with

the ChIP antibodies for H3K27ac (Abcam), at 4^{o}C overnight with rotation. The following day, immunocomplexes containing antibody/protein/DNA were incubated with Protein Agarose A beads at 4^{o}C for 2~4 hours. Immunocomplexes were washed with low salt, high salt, LiCl and TE buffer. Complexes were incubated with elution buffer (0.1M NaHCO3) at room temperature for 15 mins with rotation. After centrifuging at 2000 rpm for 2 mins at room temperature, the supernatant was transferred to new fresh tube. After repeating the elution step, 25 µl of 4M NaCl was added to 500 µl of supernatant to reverse cross-links at 65^{o}C overnight. The next day, DNA was purified using phenol-chloroform extraction, and resuspended in nuclease free water and analyzed by qPCR. SYBR green master mix (Applied Biosystems) was used to measure amplification of DNA using 7500 Fast Real-Time PCR system (Applied Biosystems). After normalization to the Input DNA, the amount of output DNA of each target protein was calculated by subtracting that of the IgG control. ChIP antibodies and primer sequences are listed in Table E3.

RNA-sequencing library preparation and sequencing.

cDNA libraries were prepared with 1 ng of RNA per sample using Clontech SMART-Seq v4 Ultra Low Input RNA Kit (TaKaRa). Libraries were sequenced with 2×75bp paired-end configuration on HiSeq4000 (Illumina) using HiSeq 3000/4000 PE SBS Kit. A Phred quality score (Q score) was used to measure the quality of sequencing. More than 90% of the sequencing reads reached Q30 (99.9% base call accuracy).

RNA-Sequencing alignment and analysis.

The sequencing data were first assessed using FastQC (Babraham Bioinformatics) for quality control. All sequenced libraries were then mapped to the mouse genome (UCSC mm10) using STAR RNA-seq aligner (24). The reads distribution across the genome was assessed using bamutils (from ngsutils) (25). Uniquely mapped sequencing reads were assigned to mm10 refGene genes using featureCounts (26). Differential expression analyses were performed using edgeR v3.22.3 implemented in the Bioconductor package (27) to identify differentially expressed mRNAs between $ST2^+$ and $ST2^-$ samples. Biological coefficients of variation between the samples were estimated using an empirical Bayes approach under the assumption that the data follows a negative binomial distribution. We filtered out low expression transcripts based on percentage of samples (less than 50%) and CPM cutoff of 0.5. A total of 14,943 mRNAs remained after filtering and used in the differential expression analysis by edgeR. Statistical significance was defined as FDR p-value ≤0.05 and a fold change (FC) ≥2 of expression level between comparison of knockout mice and controls. The heat map and locus-by-locus volcano plot were performed using R package. Gene set enrichment analysis (GSEA) (28) was used for the whole genome functional enrichment analysis, based on annotation files from Molecular Signatures Database (MSigDB) immunologic gene sets, to identify biological pathways that were significantly enriched after 3,000 times permutation.

Heatmap generation and functional enrichment

For visualizing the expression data obtained from the RNA-seq analysis, heatmaps were generated. Normalized counts for the most differentially expressed genes (p-value<0.05 and FDR<0.05) between $ST2^+$ and $ST2^-$ Treg cell subtypes were given as input to generate clustered

heatmaps based on functional themes using the Morpheus platform (29) and heatmapper (30). Ontology analysis of genes was performed using gProfiler (31) to generate summaries of the enriched biologic processes.

Results

Tfr-deficiency results in exacerbated airway inflammation

To define the regulatory effects of Bcl6-deficiency on allergic airway inflammation, WT, and *Bcl6*$^{fl/fl}$ mice crossed to either Foxp3-cre or CD4-cre transgenic mice, previously shown to lack Bcl6 in specific cell populations (2, 32-38), were exposed to HDM extract every other day for 16 days (Fig 1a). Tfr cell populations were decreased in the mLN of *Bcl6*$^{fl/fl}$ Foxp3-cre mice consistent with a previous report (32) in the absence of altered Treg cell populations (Fig 1b, 1c, Figure E1a). Unexpectedly, Tfh and GC B cell populations were also significantly decreased in *Bcl6*$^{fl/fl}$ Foxp3-cre mice (Fig 1d-1g). Despite a marked decrease in GC B cells, *Bcl6*$^{fl/fl}$ Foxp3-cre mice produced increased concentrations of HDM-specific IgE and total IgE compared to WT mice (Fig 1h). *Bcl6*$^{fl/fl}$ CD4-cre mice do not produce IgE due to the lack of a GC response (Fig 1d-1h). The numbers of total cells, eosinophils, neutrophils, total CD4^{+} T cells and Th2 cytokine-producing T cells in the bronchoalveolar lavage (BAL) were significantly increased in *Bcl6*$^{fl/fl}$ Foxp3-cre mice compared to WT and *Bcl6*$^{fl/fl}$ CD4-cre mice (Fig 1i, j, Figure E1b, e). Similar to the BAL, *Bcl6*$^{fl/fl}$ Foxp3-cre mice showed increased total cells and Th2 cytokine-producing T cells in lung tissue (Fig 1k, Figure E1c, e). However, the number of IL-10 producing T cells in BAL and lung was similar between the two conditional mutant strains (Figure E1d). Consistent with a previous report (23), *Bcl6*$^{fl/fl}$ CD4-cre mice have comparable numbers of BAL cells with WT mice, but increased inflammation in lung tissue (Fig. 1i, k) despite impaired IgE production. These data indicated that the lack of Bcl6 in Foxp3-expressing cells resulted in dysregulated type 2 responses and exacerbated airway inflammation.

Bcl6-deficiency in Treg cells leads to increased ST2^{+} Treg cell development

The mechanism for increased airway inflammation in *Bcl6*$^{fl/fl}$ Foxp3-cre mice was unclear. A previous report demonstrated that Bcl6-deficient splenic Treg cells expressed more *Il1rl1*, encoding the IL-33 receptor ST2, than WT Treg (22). Moreover, recent studies revealed that ST2$^+$ Treg cells in the lung lost their suppressive function and promoted severe airway inflammation in response to IL-33 treatment (39). Therefore, we hypothesized that *Bcl6*$^{fl/fl}$ Foxp3-cre mice might have more ST2$^+$ Treg cells that could be responsible for exacerbated airway inflammation. To test this, we analyzed ST2$^+$ Treg cells in lung and mLN from HDM challenged mice. Interestingly, both *Bcl6*$^{fl/fl}$ Foxp3-cre and CD4-cre mice have significantly greater percentages of the ST2$^+$ Treg cell population in Treg or total CD4$^+$ T cell populations than WT mice (Fig 2a, b). There is an increase in the overall Treg population in the lung in *Bcl6*$^{fl/fl}$ Foxp3-cre mice compared to wild type mice, that includes an increase in the ST2$^-$ Treg population (Fig 2c). Moreover, ST2 expression in considerably higher on ST2$^+$ Tregs from *Bcl6*$^{fl/fl}$ Foxp3-cre mice, compared to those from wild type mice (Fig 2d). ST2$^+$ Treg cells are highly activated and ST2 expression is enhanced by *Gata3* (40-43). We confirmed higher *Gata3* expression in lung- and mLN ST2$^+$ Treg cells and an activated phenotype marked by increased expression of CD44 and decreased expression of CD62L, compared to ST2$^-$ Tregs (Figure E2a-c).

Consistent with data in Figure 1j and k, ST2$^+$ conventional T cells (Tconv) that include Th2 cells in both lung and mLN were increased in *Bcl6*$^{fl/fl}$ Foxp3-cre and CD4-cre mice (Fig 2e, f). Increased ST2$^+$ Treg cell populations in lung and mLN of *Bcl6*$^{fl/fl}$ Foxp3-cre mice developed in the absence of altered ST2$^+$ Tconv cells, and this effect of Bcl6-deficiency in Foxp3-expressing cells was also detected in unchallenged mice (Figure E2d). Importantly, in wild type mice, Bcl6 expression is mutually exclusive to the ST2$^+$ Treg population (Figure E2e, f). *Bcl6*$^{fl/fl}$ Foxp3-cre mice had increased ST2$^+$ Treg cells and ST2$^+$ Tconv cell population in mesLN

compared to wild type mice (Figure E2g), suggesting the effects of Bcl6-deficiency on the $ST2^+$ Treg population were systemic. The majority of $ST2^+$ Treg cells in lung express Helios, suggesting that most $ST2^+$ Treg cells are thymus-derived Treg cells (Figure E2h). These data suggest that Bcl6 negatively regulates $ST2^+$ Treg cell development and that in the absence of Bcl6 there is an accumulation of $ST2^+$ Treg cells in the lung during allergic airway inflammation.

Next, we tested whether $ST2^+$ Treg cell development varies with genetic background, by comparing $ST2^+$ Treg generation in HDM challenged C57BL/6 and BALB/c mice, the latter more susceptible to allergic inflammation (44, 45). While the number of $ST2^+$ Treg and Tconv cells in lung were significantly higher in BALB/c mice, the percentages of these cell types were similar between groups (Figure E3a). The number and percentage of $ST2^+$ Treg and Tconv cells in mLN were similar between groups (Figure E3b). In spite of difference in the number of $ST2^+$ Treg and Tconv cells in the lung, fold changes of the number of total lung and mLN cells after HDM challenge were similar between groups (Figure E3c), suggesting that the development and function of $ST2^+$ Treg cells are independent of genetic background.

Pro-inflammatory transcriptional profile of $ST2^+$ Treg cells in allergic airway inflammation

To further define the phenotype of $ST2^+$ Treg cells in the mLN that develop in the allergic airway model, we sorted Treg cells from mLN of HDM challenged WT mice based on the expression of YFP (Foxp3-reporter) and activation markers to identify Tfr cells ($CXCR5^+$ $PD\text{-}1^+$), $ST2^+$ Treg cells ($CD44^{high}$ and $CD62L^{low}$ $ST2^+$), $ST2^-$ Treg cells ($CD44^{high}$ and $CD62L^{low}$ $ST2^-$), and naïve Treg cells ($CD44^{low}$ and $CD62L^{high}$). In Tfr cells, there is a high ratio of *Bcl6* to *Prdm1* (encoding Blimp1) expression that is reversed in $ST2^+$ Treg cells (Fig 3a). We

confirmed the Bcl6 gene expression pattern by protein expression (Fig 3b). This is similar to the correlation between Blimp1 and ST2 expression in visceral adipose tissue (VAT) Treg cells (46). Expression of *Bach2*, a repressor of inflammatory cytokine expression in Treg cells (47, 48), was decreased in $ST2^+$ Treg cells. However, the enhanced *Foxp3* expression in $ST2^+$ Treg cells suggested that these cells are not intrinsically unstable. *Ccr7*, encoding a chemokine receptor for homing to secondary lymphoid organs (49, 50), and *Cxcr3*, encoding a chemokine receptor for migrating to sites of type1 inflammation (51, 52), were significantly decreased in $ST2^+$ Treg cells compared to $ST2^-$ Treg cells (Fig 3a). CCR8-expressing Treg cells are capable of migrating to sites of Th2 cell-mediated inflammation (53), and *Ccr8* mRNA was significantly enriched in $ST2^+$ Treg cells. Importantly, Th2 cytokine genes were enriched in $ST2^+$ Treg cells (Fig 3c). While *Il4* expression was greatest in Tfr cells, $ST2^+$ Treg cells still express *Il4* in greater amounts than other Treg subsets. Thus, $ST2^+$ Tregs acquire a profile associated with type 2 inflammation.

To further explore the $ST2^+$ Treg cell signature in allergic airway inflammation, we performed RNA-seq on sorted $ST2^+$ and $ST2^-$ Treg cells isolated from lung. We observed significant differences in the gene expression patterns between the two $Foxp3^+$ populations (Fig 3d). Among significant differences in the $ST2^+$ population were increased type 2 cytokines and transcription factors, and decreased expression of genes encoding RORγt and T-bet (Fig 3e, left). We confirmed increased Th2 cytokine production in $ST2^+$ Treg cells in protein level (Figure E4a). We observed similar patterns of differential gene expression when we analyzed $ST2^+$ and $ST2^-$ Treg cells isolated from the lung by qRT-PCR (Figure E4b-4d). Gene set enrichment analysis identified the VAT Treg signature in the $ST2^+$ Treg cells (Fig 3f). Indeed, there was a clear distinction in the transcriptional signatures of $ST2^+$ and $ST2^-$ Treg cells that respectively aligned with VAT Treg cells and peripheral Treg cells (Fig 3e, right). Ontology analysis of genes

enrichment in $ST2^+$ Treg cells revealed that $ST2^+$ Treg cells are more sensitive to environmental cytokines and produce effector cytokines during airway inflammation (Fig 3g). Together, these data demonstrate that $ST2^+$ Tregs in the context of allergic lung inflammation have a pro-type 2 inflammatory phenotype and share a genetic signature with VAT Tregs.

Bcl6 inhibits and Blimp1 promotes ST2 expression in Treg cells

To directly test whether Bcl6 is a negative regulator of $ST2^+$ Treg cell development, splenic Treg cells from WT and *Bcl6*$^{fl/fl}$ Foxp3-cre mice were sorted and stimulated in the presence or absence of IL-33 for 3 days. Treatment with IL-33 significantly increased the frequency of $ST2^+KLRG1^+$ Tregs in WT and Bcl6-deficient cultures (Fig 4a-c). The induction of ST2 and KLRG1 on Tregs by IL-33 is consistent with previous reports (40-43), and double positive Tregs were more prevalent in resting or IL-33-treated Bcl6-deficient cultures. Interestingly, IL-33 treatment decreased *Bcl6* expression while increasing *Prdm1* expression (Fig 4d). Similar to ex vivo Treg cells, in vitro Treg (iTreg) cells cultured with IL-33 displayed increased *Il1rl1* expression while concomitantly decreasing *Bcl6* mRNA (Figure E5a, b). Bcl6-deficient iTreg expressed greater *Il1rl1* than in WT iTreg under all conditions. We then tested whether the $ST2^+$ Treg cell population responded to exogenous IL-33 by intranasal challenge. In WT and *Bcl6*$^{fl/fl}$ Foxp3-cre mice there was a significant increase of $ST2^+$ Treg cells recovered from the lungs compared to untreated mice, and a significantly higher percentage in *Bcl6*$^{fl/fl}$ Foxp3-cre mice, compared to WT mice (Fig 4e). We then sorted $ST2^+$ and $ST2^-$ Treg cells from IL-33-treated WT mice and observed enriched *Gata3* expression in $ST2^+$ Treg cells and enriched *Bcl6* expression in $ST2^-$ Treg cells (Figure E5c). Bcl6-deficient splenic Treg cells did not produce Th2 cytokines in the absence of IL-33 signaling despite expressing comparable levels of

Gata3 in the presence or absence of IL-33 signaling (Figure E5d). Treatment of ex vivo Treg cells with IL-33 increased the H3K27ac modification at the *Il1rl1* and *Prdm1* gene loci (Figure E5e-f). These data suggest that the IL-33/ST2 signaling pathway promotes $ST2^+$ Treg cell development by suppressing Bcl6 and promoting Blimp1 expression. Consistent with a previous report (40), Gata3 expression was not altered after IL-33 treatment but was increased in Bcl6 deficient Treg cells, compared to wild type cells, irrespective of IL-33 treatment (Fig 4d). IL-33 treatment of ex vivo Treg cells from BALB/cJ and C57BL/6 mice showed comparable $ST2^+$ Treg cell development (Figure E5g, h). Overall, these data suggest that Bcl6 negatively regulates $ST2^+$ Treg cell development by repressing the expression of the $ST2^+$ Treg cell promoting transcription factors *Prdm1* and *Gata3*.

Naïve *Il33*$^{-/-}$ mice have normal $ST2^+$ Treg cell numbers and populations in both lymphoid and non-lymphoid tissues (41). Based on that data, IL-33 may be dispensable for generation of $ST2^+$ Treg cells (41). Similarly, IL-33 failed to induce ST2 expression in $ST2^-$ Treg cells (42). We then explored potential drivers of $ST2^+$ Treg cell development. The IL-2/STAT5 pathway is critical for development and maintenance of Treg cells (54-58) and the IL-2/STAT5/Blimp-1 axis represses Tfr cell development by inhibiting Bcl6 expression (59). In addition to Bcl6 antagonistic functions (5, 59), the preferential expression of Blimp1 in $ST2^+$ Treg cells suggested that Blimp1 might be a key player. To directly test this, we stimulated splenic Treg cells from WT and *Prdm1*$^{fl/fl}$ Foxp3-cre mice with or without IL-33 for 3 days. Interestingly, Blimp1-deficiency nearly eliminated the $KLRG1^+$ population and significantly reduced the $ST2^+$ population in basal and IL-33-treated conditions (Fig 4f-h). Consistent with the in vitro results, Blimp1-deficient mice have impaired $ST2^+$ Treg cell percentages in naïve mice and had reduced $ST2^+$ Treg cells during HDM induced airway inflammation (Fig 4i). Moreover, Bcl6-expressing

Treg cells in lung were increased in Blimp1-deficient mice (Figure E5i). We confirmed the positive effects of Blimp-1 deficiency on Tfr cell development in mLN (2) (Figure E5j, k). These data suggest that Blimp1 positively regulates $ST2^+$ Treg cell development, possibly by antagonizing Bcl6 expression.

Bcl6-deficient $ST2^+$ Treg cells promote airway inflammation

To discriminate the effects of Bcl6-deficiency in Tregs and Tconv (which are not Bcl6-deficient in *Bcl6*$^{fl/fl}$ Foxp3-cre mice), we adoptively transferred sorted lung $ST2^+$ Treg or Tconv cells from wild type or *Bcl6*$^{fl/fl}$ Foxp3-cre mice HDM-challenged mice to naïve wild type recipient mice. After three challenges with HDM, we analyzed the number of inflammatory cells in BAL and lung (Fig 5a). Interestingly, although the total numbers of BAL cells were similar among groups, indicative of the acute challenge (Fig 5b), mice that received Bcl6-deficient $ST2^+$ Treg cells had the greatest increases in the number of lung cells, neutrophils, eosinophils and $CD4^+$ T cells while wild type $ST2^+$ Treg cell recipient mice had cell numbers comparable with PBS control (Fig 5c-d). Transferred $ST2^+$ Tconv cells did not induce inflammation. In Bcl6-deficient ST2+ Treg cell recipient mice, the vast majority of ST2+ donor cells were Foxp3+ though a subpopulation lost Foxp3 expression, suggesting that Bcl6-deficient Tregs might be unstable in this model (Fig 5e) (60). These data suggest that Bcl6 plays important roles in regulating both development and function of $ST2^+$ Treg cells which directly mediate airway inflammation.

Although the mechanistic basis of the capacity of Bcl6-deficient ST2+ Treg to mediate inflammation is unclear, it is likely linked to greater expression of ST2 itself (Fig 2d), and the effects of Bcl6 on expression of ST2+ Treg cell effector molecules (63) that include *Areg*, *Lilrb4*,

and *Ccl3*, but not type 2 cytokines such as *Il5* and *Il13* (Fig 5f). This suggests that the ability of Bcl6-deficient Tregs to promote inflammation, including neutrophils, is due to increased pro-inflammatory activity and chemokine production. We also observed that Bcl6-deficiency resulted in increased *Prdm1* in ST2^{-} Tregs (Fig 5f), suggesting that Blimp1 might be an important target in the acquisition of ST2 expression.

ST2-deficiency compensates for the lack of Bcl6 in Treg cells during allergic airway inflammation

In a previous study, *Il1rl1*$^{-/-}$ mice showed attenuated allergic airway inflammation with impaired GATA3^{+} Th2-like Treg cell development (39). The authors suggested that ST2 is indispensable for Th2-like Treg cell development. In parallel, our data indicate that ST2 is important for IL-33-mediated Bcl6 repression. Therefore, we questioned whether ST2-deficiency would limit the effects of Bcl6-deficiency in Treg cells during allergic airway inflammation. To answer this question, we generated *Il1rl1*$^{-/-}$*Bcl6*$^{fl/fl}$ Foxp3-cre mice and induced HDM airway inflammation. As expected, ST2 expression was not detected on Tregs or Tconv cells in either *Il1rl1*$^{-/-}$ or *Il1rl1*$^{-/-}$*Bcl6*$^{fl/fl}$ Foxp3-cre mice (Figure E6a). ST2-deficient mice also had a defect in the generation of Tfh, Tfr, and GC B cell development (Fig 6a). Importantly, ST2-deficiency did not compensate for the lack of Bcl6 in the Tfr cell population and the Tfr population in *Il1rl1*$^{-/-}$ *Bcl6*$^{fl/fl}$ Foxp3-cre mice was similar to *Bcl6*$^{fl/fl}$ Foxp3-cre mice, but significantly less than control mice (Fig. 6a). Accordingly, the increased total and antigen-specific IgE that resulted from Tfr cell-deficiency was not compensated by simultaneous deficiency in ST2 (Fig 6b). These results suggested that *Il1rl1*$^{-/-}$*Bcl6*$^{fl/fl}$ Foxp3-cre mice maintain the effects of Tfr-deficiency and provided

the opportunity to assess the loss of IL-33 responsiveness on the increased allergic airway inflammation in *Bcl6*$^{fl/fl}$ Foxp3-cre mice.

To test this we analyzed airway inflammation and observed that *Il1rl1*$^{-/-}$ and *Il1rl1*$^{-/-}$ *Bcl6*$^{fl/fl}$ Foxp3-cre mice have comparable numbers of BAL and lung cells with WT mice (Fig 6c, 6d). IL-13-producing CD4^{+} and GATA3^{+} Tconv cells were significantly decreased in *Il1rl1*$^{-/-}$ *Bcl6*$^{fl/fl}$ Foxp3-cre mice compared to *Bcl6*$^{fl/fl}$ Foxp3-cre mice and restored to those observed in WT mice (Fig 6e, 6f). Despite diminished inflammation and Th2 cytokine production, lung Treg cells from *Il1rl1*$^{-/-}$*Bcl6*$^{fl/fl}$ Foxp3-cre mice express more GATA3 than Treg cells from WT mice (Fig 6g), suggesting that Bcl6 is required for Gata3 repression. Importantly, the percentage of cells that are Foxp3^{+} KLRG1^{+}, a surrogate for ST2 since the majority of KLRG1^{+} Treg cells are also ST2^{+}, were similar in the absence ST2 (Figure E6b-c). This suggests that the diminished inflammation in *Il1rl1*$^{-/-}$ and *Il1rl1*$^{-/-}$*Bcl6*$^{fl/fl}$ Foxp3-cre mice is due to the lack of ST2 but not the lack of a Treg cell compartment. Together, these data suggest that the absence of ST2 attenuates the exacerbated allergic airway inflammation that occurs in mice with Bcl6-deficient Treg cells and distinguishes the effects of Bcl6 in Tfr cells from the effects in Treg cells that control allergic inflammation.

Discussion

Bcl6-expressing Tfr cells are important for the humoral immune response through regulation of germinal center reactions (8-10). Depending on the inflammatory milieu, Tfr cells can function as repressors or helpers of the GC reaction (18). Dysregulated functions of Tfr cells can lead to autoimmune diseases (61). Yet, the function of Bcl6 in regulatory T cells in the context of allergic airway inflammation is not fully understood. In this report, we have defined critical roles for Tfr cells in regulating the production of antigen specific IgE in an HDM extract induced airway inflammation model. This observation confirms a recent report that made similar observations on the function of Tfr in controlling IgE using a distinct genetic model (62).

Our report defines an additional role for the balance of Bcl6 and Blimp-1 activity in Treg cells. Bcl6 represses and Blimp-1 activates ST2 expression in Treg cells in a cell-intrinsic manner. The adoptive transfer studies highlight the cell-intrinsic nature of this phenomenon since Bcl6 is only deleted in Foxp3-expressing cells in this model and would not impact the function of conventional T cells. The data suggest that Bcl6 is important in $ST2^-$ Treg cells to maintain the $ST2^-$ phenotype. In the absence of Bcl6, Blimp-1 expression is increased and there is an increase in the percentage of $ST2^+$ Treg cells, and an increase in the amount of ST2 expressed per Treg cell. The $ST2^{hi}$ Treg cells would be more sensitive to an allergic environment and with increased expression of other effector molecules, Bcl6-deficient Tregs are potent at promoting allergic inflammation. The ability of Bcl6-deficient Tregs to recruit additional effectors of allergic inflammation further amplifies this activity. It is also possible that increased ST2 expression decreases the stability of the Treg cells and an inflammatory environment converts them into ST2+ Tconv cells that could also potentially impact the generation of inflammation.

There has been significant characterization of the ST2-expressing Treg population in the colon and lung (40, 41, 43). $ST2^+$ Treg cells are highly activated Th2-like Treg cells that retain Foxp3 expression and have increased GATA3 and production of Th2 cytokines in response to IL-33. IL-33 enhances the differentiation, accumulation and maintenance of $ST2^+$ Treg in inflamed tissues (40-42). $ST2^+$ Treg cells are effective in suppressing Th1 or Th17 cell inflammation in a colitis model and T cell proliferation, but fail to suppress, and potentially exacerbate, Th2 type responses in an allergic airway disease model (39, 40, 63). In support of a key role for Bcl6 in controlling this Treg population, Treg cells from germline *Bcl6*-deficient mice have increased ST2 expression, suppress Th1/Th17 cell-driven colitis, inhibit T cell proliferation, but promote Th2 type allergic airway inflammation (22). Human $ST2^+$ Treg cells are found in the skin of systemic sclerosis patients (64). Similar to murine $ST2^+$ Treg cells, these human $ST2^+$ Treg cells and in vitro cultured human Treg cells produce Th2 cytokines in response to IL-33 (64, 65). Moreover, human Treg cells from HDM-sensitized asthmatic children have suppressive function on Th1 cells but fail to suppress allergen-specific Th2 cytokine expression and amplify Th2 cytokines in response to IL-33 (66). However, the mechanisms controlling $ST2^+$ Treg cell development are still not fully defined.

In the RNA-seq analysis we identified a transcriptional signature associated with the $ST2^+$ Treg cells in allergic lung inflammation. There is an enrichment of genes associated with type 2 immunity in the $ST2^+$ Treg population, while genes associated with type 1 and type 17 immunity are enhanced in the $ST2^-$ Treg cells. There is remarkable overlap between the transcriptional signature in the allergic $ST2^+$ Treg cells and the VAT $ST2^+$ Treg cells, adipose tissue resident Treg cells. While VAT $ST2^+$ Treg cells maintain insulin sensitivity through control of inflammation in adipose tissue (67), $ST2^+$ Treg cells in lung promote allergic airway

inflammation (39). The function of VAT ST2$^+$ Tregs might also be to promote modest type 2 inflammation, and we have not examined whether this might be amplified in the *Bcl6* $^{fl/fl}$ Foxp3-Cre mice. It also remains to be tested whether ST2$^+$ Tregs might control cellular metabolism in the lung. The development and accumulation of VAT Treg cells depend on PPAR-γ which is regulated by the IL-33/ST2 pathway and mediated by IRF4 and BATF expression (46). The IL-33/ST2 pathway subsequently activates GATA3 leading to expansion of ST2$^+$ Treg cells and expression of Th2 cytokines (40, 41). However, naïve *Il33*-deficient mice develop ST2$^+$ Treg cells (41), suggesting that there are unidentified signaling pathways for ST2$^+$ Treg cell development. In this study, we defined Blimp1 as a key player for ST2$^+$ Treg cell development. ST2 is preferentially expressed in Blimp1$^+$ Treg cells (46), and we confirmed preferential expression of Blimp1 in ST2$^+$ Treg cells. Blimp1-deficiency impairs ST2$^+$ Treg cell development in vitro and in vivo. While there is a decreased number of ST2$^+$ Treg cells in *Prdm1* $^{fl/fl}$ Foxp3-Cre mice, these mice have comparable airway inflammation to WT mice (data not shown). This observation could be due to several reasons including Blimp1 playing a critical role in the functions of Treg cells (68), and that Th2 cytokine production is already very low in wild type Tregs and cannot be lowered further by the absence of Blimp1. Blimp1 is a well-known repressor of Bcl6 transcription, and increased Bcl6 expression in Blimp1-deficient Treg cells likely contributes to the decreased development of ST2$^+$ Treg cells from Blimp1-deficient Treg cells. Bcl6 negatively regulates a subset of genes associated with the ST2$^+$ Treg subset including *Prdm1* and *Il1rl1*, both of which contribute to the ST2$^+$ Treg phenotype. Thus, Bcl6 and Blimp1 are reciprocal regulators of Treg cell fate, similar to their reciprocal regulation of T helper cell and –B cell differentiation.

The functions of Bcl6 in regulating type 2 responses are complex. One of the first observations in *Bcl6*$^{-/-}$ mice was an increased Th2 responses (19, 20). However, this occurs through Bcl6 function in a number of cell types. One potential mechanism is through the repression of GATA3 which has been observed in conventional and regulatory T cells (22, 69). In our studies using mice that lacked Bcl6 specifically in Foxp3-expressing cells, we did not observe differences in GATA3 and ST2 expression in the ST2^{+} Treg population. Rather, we observed expansion of the ST2^{+} Treg population. Moreover, adoptively transferred Bcl6-deficient ST2^{+} Treg cells induced airway inflammation in recipient mice after limited challenges, while ST2^{+} Bcl6-deficient Tconv or either subset of wild type ST2^{+} T cells did not. These data suggest that Bcl6 is important for the suppressive function of ST2^{+} Treg cells, and this study provides a first step to defining the mechanism. As deletion of ST2 normalized the increased Th2 inflammation observed in the Bcl6$^{fl/fl}$ Foxp3-Cre mice, it suggests that the IL-33/ST2 pathway represents a major Bcl6 target that contributes to the control of allergic inflammation.

The effects of ST2-deficiency can vary with the model examined. In our study, ST2 deficiency did not alter overall inflammation or Th2 cells compared to control mice. In the Ova/Alum model, ST2-deficient mice developed attenuated airway inflammation that was linked to impaired DC activation (70). In the HDM model, ST2-deficient mice showed varying phenotypes depending on the dose of HDM, sensitization protocol, and analysis time point after last challenge. In a chronic HDM model, reduced airway remodeling, AHR and airway inflammation were observed in ST2-deficient mice (71). However, in another HDM model, TSLP and IL-25 compensate for the loss of ST2 and diminished Th2 cells by expanding ILC2 (72, 73). Thus, the effects of IL-33 signaling are sensitive to the context of the response. Regardless, the lack of a phenotype of ST2-deficiency in our studies allowed us to examine the

554 effects in the context of cell-specific Bcl6-deficiency. ST2-deficiency in our studies resulted in
555 decreased germinal center responses. This could be linked to the effects of ST2-deficiency on
556 DC function (70, 74), rather than an intrinsic effect in Tfr cells.

557 Our studies further define the complex roles of Tfr cells in regulating antibody responses,
558 particularly IgE. Tfr cell-deficiency did not alter influenza-specific IgG production in an
559 influenza infection model (59, 61). However, Tfr cells suppress antigen specific B cell function
560 in several models (8-10). In our HDM induced airway inflammation model, Treg-specific Bcl6
561 deficient mice (*Bcl6*$^{fl/fl}$ Foxp3-cre) similarly have reduced Tfr cell numbers but produced higher
562 concentrations of HDM-specific IgE and total IgE than WT mice while producing comparable
563 HDM specific IgG1. These data suggest that Tfr cells function as a repressor of IgE production.
564 A recent report suggested that Tfr cells also limit allergic inflammation using an approach to
565 delete Foxp3- and Cxcr5-expressing cells (62). This raises another important aspect of these two
566 models in comparing the deletion of Tfr cells versus the loss of Tfr and other Treg functions by
567 genetic deletion of Bcl6. Importantly, the effects of Bcl6 in the Tfr and Treg compartments are
568 distinguished by the effects of ST2-deficiency, as Tfr cells are ST2^{-}. Comparing these and other
569 models will be required to refine the distinct function of Tfr and ST2^{+} Treg cells.

570 In this report we have defined specific functions for Bcl6 in the Foxp3-expressing CD4^{+}
571 T cell subset (Fig 7). In the context of HDM-induced allergic airway inflammation, Bcl6 is
572 required for Tfr cells to develop and repress IgE production. In Treg cells, Bcl6 represses ST2,
573 Gata3 and Blimp1, and in the absence of Bcl6 there is an expansion of the ST2^{+} Treg population,
574 increased Th2 cell development, and increased allergic airway inflammation. Importantly, co-
575 deficiency of ST2 and Bcl6 distinguishes these two activities of Bcl6 in Foxp3-expressing cells
576 by normalizing the airway inflammation without having an effect on the production of IgE. The

577 presence of the KLRG1^{+} Treg population in the ST2-deficient mice suggests that impact is
578 specifically from IL-33 signaling, rather than a loss of the entire population. Each of these
579 functions will be important to understand the detailed mechanisms of allergic airway
580 inflammation.
581
582

583 References

584 1. Basso K, Dalla-Favera R. BCL6: master regulator of the germinal center reaction and key
585 oncogene in B cell lymphomagenesis. Adv Immunol. 2010;105:193-210.
586 2. Xie MM, Koh BH, Hollister K, Wu H, Sun J, Kaplan MH, et al. Bcl6 promotes follicular helper T-cell
587 differentiation and PD-1 expression in a Blimp1-independent manner in mice. Eur J Immunol.
588 2017;47(7):1136-41.
589 3. Hatzi K, Nance JP, Kroenke MA, Bothwell M, Haddad EK, Melnick A, et al. BCL6 orchestrates Tfh
590 cell differentiation via multiple distinct mechanisms. J Exp Med. 2015;212(4):539-53.
591 4. Nurieva RI, Chung Y, Martinez GJ, Yang XO, Tanaka S, Matskevitch TD, et al. Bcl6 mediates the
592 development of T follicular helper cells. Science. 2009;325(5943):1001-5.
593 5. Johnston RJ, Poholek AC, DiToro D, Yusuf I, Eto D, Barnett B, et al. Bcl6 and Blimp-1 are
594 reciprocal and antagonistic regulators of T follicular helper cell differentiation. Science.
595 2009;325(5943):1006-10.
596 6. Yu D, Rao S, Tsai LM, Lee SK, He Y, Sutcliffe EL, et al. The transcriptional repressor Bcl-6 directs T
597 follicular helper cell lineage commitment. Immunity. 2009;31(3):457-68.
598 7. Yu RY, Wang X, Pixley FJ, Yu JJ, Dent AL, Broxmeyer HE, et al. BCL-6 negatively regulates
599 macrophage proliferation by suppressing autocrine IL-6 production. Blood. 2005;105(4):1777-84.
600 8. Wollenberg I, Agua-Doce A, Hernandez A, Almeida C, Oliveira VG, Faro J, et al. Regulation of the
601 germinal center reaction by Foxp3+ follicular regulatory T cells. J Immunol. 2011;187(9):4553-60.
602 9. Linterman MA, Pierson W, Lee SK, Kallies A, Kawamoto S, Rayner TF, et al. Foxp3+ follicular
603 regulatory T cells control the germinal center response. Nat Med. 2011;17(8):975-82.
604 10. Chung Y, Tanaka S, Chu F, Nurieva RI, Martinez GJ, Rawal S, et al. Follicular regulatory T cells
605 expressing Foxp3 and Bcl-6 suppress germinal center reactions. Nat Med. 2011;17(8):983-8.
606 11. Crotty S, Johnston RJ, Schoenberger SP. Effectors and memories: Bcl-6 and Blimp-1 in T and B
607 lymphocyte differentiation. Nat Immunol. 2010;11(2):114-20.
608 12. Fazilleau N, Mark L, McHeyzer-Williams LJ, McHeyzer-Williams MG. Follicular helper T cells:
609 lineage and location. Immunity. 2009;30(3):324-35.
610 13. Linterman MA, Rigby RJ, Wong RK, Yu D, Brink R, Cannons JL, et al. Follicular helper T cells are
611 required for systemic autoimmunity. J Exp Med. 2009;206(3):561-76.
612 14. Odegard JM, Marks BR, DiPlacido LD, Poholek AC, Kono DH, Dong C, et al. ICOS-dependent
613 extrafollicular helper T cells elicit IgG production via IL-21 in systemic autoimmunity. J Exp Med.
614 2008;205(12):2873-86.
615 15. Vinuesa CG, Cook MC, Angelucci C, Athanasopoulos V, Rui L, Hill KM, et al. A RING-type ubiquitin
616 ligase family member required to repress follicular helper T cells and autoimmunity. Nature.
617 2005;435(7041):452-8.
618 16. Sage PT, Alvarez D, Godec J, von Andrian UH, Sharpe AH. Circulating T follicular regulatory and
619 helper cells have memory-like properties. J Clin Invest. 2014;124(12):5191-204.
620 17. Sage PT, Paterson AM, Lovitch SB, Sharpe AH. The coinhibitory receptor CTLA-4 controls B cell
621 responses by modulating T follicular helper, T follicular regulatory, and T regulatory cells. Immunity.
622 2014;41(6):1026-39.
623 18. Laidlaw BJ, Lu Y, Amezquita RA, Weinstein JS, Vander Heiden JA, Gupta NT, et al. Interleukin-10
624 from CD4(+) follicular regulatory T cells promotes the germinal center response. Sci Immunol.
625 2017;2(16).
626 19. Dent AL, Hu-Li J, Paul WE, Staudt LM. T helper type 2 inflammatory disease in the absence of
627 interleukin 4 and transcription factor STAT6. Proc Natl Acad Sci U S A. 1998;95(23):13823-8.

628 20. Dent AL, Shaffer AL, Yu X, Allman D, Staudt LM. Control of inflammation, cytokine expression,
629 and germinal center formation by BCL-6. Science. 1997;276(5312):589-92.
630 21. Ye BH, Cattoretti G, Shen Q, Zhang J, Hawe N, de Waard R, et al. The BCL-6 proto-oncogene
631 controls germinal-centre formation and Th2-type inflammation. Nat Genet. 1997;16(2):161-70.
632 22. Sawant DV, Sehra S, Nguyen ET, Jadhav R, Englert K, Shinnakasu R, et al. Bcl6 controls the Th2
633 inflammatory activity of regulatory T cells by repressing Gata3 function. J Immunol. 2012;189(10):4759-
634 69.
635 23. Kobayashi T, Iijima K, Dent AL, Kita H. Follicular helper T cells mediate IgE antibody response to
636 airborne allergens. J Allergy Clin Immunol. 2017;139(1):300-13 e7.
637 24. Dobin A, Davis CA, Schlesinger F, Drenkow J, Zaleski C, Jha S, et al. STAR: ultrafast universal RNA-
638 seq aligner. Bioinformatics. 2013;29(1):15-21.
639 25. Breese MR, Liu Y. NGSUtils: a software suite for analyzing and manipulating next-generation
640 sequencing datasets. Bioinformatics. 2013;29(4):494-6.
641 26. Liao Y, Smyth GK, Shi W. featureCounts: an efficient general purpose program for assigning
642 sequence reads to genomic features. Bioinformatics. 2014;30(7):923-30.
643 27. McCarthy DJ, Chen Y, Smyth GK. Differential expression analysis of multifactor RNA-Seq
644 experiments with respect to biological variation. Nucleic Acids Res. 2012;40(10):4288-97.
645 28. Subramanian A, Tamayo P, Mootha VK, Mukherjee S, Ebert BL, Gillette MA, et al. Gene set
646 enrichment analysis: a knowledge-based approach for interpreting genome-wide expression profiles.
647 Proc Natl Acad Sci U S A. 2005;102(43):15545-50.
648 29. Starruss J, de Back W, Brusch L, Deutsch A. Morpheus: a user-friendly modeling environment for
649 multiscale and multicellular systems biology. Bioinformatics. 2014;30(9):1331-2.
650 30. Babicki S, Arndt D, Marcu A, Liang Y, Grant JR, Maciejewski A, et al. Heatmapper: web-enabled
651 heat mapping for all. Nucleic Acids Res. 2016;44(W1):W147-53.
652 31. Reimand J, Kull M, Peterson H, Hansen J, Vilo J. g:Profiler--a web-based toolset for functional
653 profiling of gene lists from large-scale experiments. Nucleic Acids Res. 2007;35(Web Server issue):W193-
654 200.
655 32. Wu H, Chen Y, Liu H, Xu LL, Teuscher P, Wang S, et al. Follicular regulatory T cells repress
656 cytokine production by follicular helper T cells and optimize IgG responses in mice. Eur J Immunol.
657 2016;46(5):1152-61.
658 33. Xie MM, Dent AL. Unexpected Help: Follicular Regulatory T Cells in the Germinal Center. Front
659 Immunol. 2018;9:1536.
660 34. Xie MM, Fang S, Chen Q, Liu H, Wan J, Dent AL. Follicular regulatory T cells inhibit the
661 development of granzyme B-expressing follicular helper T cells. JCI Insight. 2019;4(16).
662 35. Hollister K, Chen Y, Wang S, Wu H, Mondal A, Clegg N, et al. The role of follicular helper T cells
663 and the germinal center in HIV-1 gp120 DNA prime and gp120 protein boost vaccination. Hum Vaccin
664 Immunother. 2014;10(7):1985-92.
665 36. Hollister K, Kusam S, Wu H, Clegg N, Mondal A, Sawant DV, et al. Insights into the role of Bcl6 in
666 follicular Th cells using a new conditional mutant mouse model. J Immunol. 2013;191(7):3705-11.
667 37. Xie MM, Liu H, Corn C, Koh BH, Kaplan MH, Turner MJ, et al. Roles of T Follicular Helper Cells and
668 T Follicular Regulatory Cells in Autoantibody Production in IL-2-Deficient Mice. Immunohorizons.
669 2019;3(7):306-16.
670 38. Wu H, Xie MM, Liu H, Dent AL. Stat3 Is Important for Follicular Regulatory T Cell Differentiation.
671 PLoS One. 2016;11(5):e0155040.
672 39. Chen CC, Kobayashi T, Iijima K, Hsu FC, Kita H. IL-33 dysregulates regulatory T cells and impairs
673 established immunologic tolerance in the lungs. J Allergy Clin Immunol. 2017;140(5):1351-63 e7.
674 40. Schiering C, Krausgruber T, Chomka A, Frohlich A, Adelmann K, Wohlfert EA, et al. The alarmin
675 IL-33 promotes regulatory T-cell function in the intestine. Nature. 2014;513(7519):564-8.

41. Siede J, Frohlich A, Datsi A, Hegazy AN, Varga DV, Holecska V, et al. IL-33 Receptor-Expressing Regulatory T Cells Are Highly Activated, Th2 Biased and Suppress CD4 T Cell Proliferation through IL-10 and TGFbeta Release. PLoS One. 2016;11(8):e0161507.
42. Matta BM, Reichenbach DK, Zhang X, Mathews L, Koehn BH, Dwyer GK, et al. Peri-alloHCT IL-33 administration expands recipient T-regulatory cells that protect mice against acute GVHD. Blood. 2016;128(3):427-39.
43. Yang J, Ramadan A, Reichenbach DK, Loschi M, Zhang J, Griesenauer B, et al. Rorc restrains the potency of ST2+ regulatory T cells in ameliorating intestinal graft-versus-host disease. JCI Insight. 2019;4(5).
44. Singh B, Shinagawa K, Taube C, Gelfand EW, Pabst R. Strain-specific differences in perivascular inflammation in lungs in two murine models of allergic airway inflammation. Clin Exp Immunol. 2005;141(2):223-9.
45. Page K, Lierl KM, Herman N, Wills-Karp M. Differences in susceptibility to German cockroach frass and its associated proteases in induced allergic inflammation in mice. Respir Res. 2007;8:91.
46. Vasanthakumar A, Moro K, Xin A, Liao Y, Gloury R, Kawamoto S, et al. The transcriptional regulators IRF4, BATF and IL-33 orchestrate development and maintenance of adipose tissue-resident regulatory T cells. Nat Immunol. 2015;16(3):276-85.
47. Kim EH, Gasper DJ, Lee SH, Plisch EH, Svaren J, Suresh M. Bach2 regulates homeostasis of Foxp3+ regulatory T cells and protects against fatal lung disease in mice. J Immunol. 2014;192(3):985-95.
48. Roychoudhuri R, Hirahara K, Mousavi K, Clever D, Klebanoff CA, Bonelli M, et al. BACH2 represses effector programs to stabilize T(reg)-mediated immune homeostasis. Nature. 2013;498(7455):506-10.
49. Forster R, Schubel A, Breitfeld D, Kremmer E, Renner-Muller I, Wolf E, et al. CCR7 coordinates the primary immune response by establishing functional microenvironments in secondary lymphoid organs. Cell. 1999;99(1):23-33.
50. Schneider MA, Meingassner JG, Lipp M, Moore HD, Rot A. CCR7 is required for the in vivo function of CD4+ CD25+ regulatory T cells. J Exp Med. 2007;204(4):735-45.
51. Hall AO, Beiting DP, Tato C, John B, Oldenhove G, Lombana CG, et al. The cytokines interleukin 27 and interferon-gamma promote distinct Treg cell populations required to limit infection-induced pathology. Immunity. 2012;37(3):511-23.
52. Koch MA, Tucker-Heard G, Perdue NR, Killebrew JR, Urdahl KB, Campbell DJ. The transcription factor T-bet controls regulatory T cell homeostasis and function during type 1 inflammation. Nat Immunol. 2009;10(6):595-602.
53. Zheng Y, Chaudhry A, Kas A, deRoos P, Kim JM, Chu TT, et al. Regulatory T-cell suppressor program co-opts transcription factor IRF4 to control T(H)2 responses. Nature. 2009;458(7236):351-6.
54. Lio CW, Hsieh CS. A two-step process for thymic regulatory T cell development. Immunity. 2008;28(1):100-11.
55. Yao Z, Kanno Y, Kerenyi M, Stephens G, Durant L, Watford WT, et al. Nonredundant roles for Stat5a/b in directly regulating Foxp3. Blood. 2007;109(10):4368-75.
56. Burchill MA, Yang J, Vogtenhuber C, Blazar BR, Farrar MA. IL-2 receptor beta-dependent STAT5 activation is required for the development of Foxp3+ regulatory T cells. J Immunol. 2007;178(1):280-90.
57. Fontenot JD, Rasmussen JP, Gavin MA, Rudensky AY. A function for interleukin 2 in Foxp3-expressing regulatory T cells. Nat Immunol. 2005;6(11):1142-51.
58. D'Cruz LM, Klein L. Development and function of agonist-induced CD25+Foxp3+ regulatory T cells in the absence of interleukin 2 signaling. Nat Immunol. 2005;6(11):1152-9.
59. Botta D, Fuller MJ, Marquez-Lago TT, Bachus H, Bradley JE, Weinmann AS, et al. Dynamic regulation of T follicular regulatory cell responses by interleukin 2 during influenza infection. Nat Immunol. 2017;18(11):1249-60.

724 60. Sawant DV, Wu H, Yao W, Sehra S, Kaplan MH, Dent AL. The transcriptional repressor Bcl6
725 controls the stability of regulatory T cells by intrinsic and extrinsic pathways. Immunology.
726 2015;145(1):11-23.
727 61. Fu W, Liu X, Lin X, Feng H, Sun L, Li S, et al. Deficiency in T follicular regulatory cells promotes
728 autoimmunity. J Exp Med. 2018;215(3):815-25.
729 62. Clement RL, Daccache J, Mohammed MT, Diallo A, Blazar BR, Kuchroo VK, et al. Follicular
730 regulatory T cells control humoral and allergic immunity by restraining early B cell responses. Nat
731 Immunol. 2019;20(10):1360-71.
732 63. Delacher M, Schmidl C, Herzig Y, Breloer M, Hartmann W, Brunk F, et al. Rbpj expression in
733 regulatory T cells is critical for restraining TH2 responses. Nat Commun. 2019;10(1):1621.
734 64. MacDonald KG, Dawson NA, Huang Q, Dunne JV, Levings MK, Broady R. Regulatory T cells
735 produce profibrotic cytokines in the skin of patients with systemic sclerosis. J Allergy Clin Immunol.
736 2015;135(4):946- e9.
737 65. Liu Q, Dwyer GK, Zhao Y, Li H, Mathews LR, Chakka AB, et al. IL-33-mediated IL-13 secretion by
738 ST2+ Tregs controls inflammation after lung injury. JCI Insight. 2019;4(6).
739 66. Reubsaet L, Meerding J, Giezeman R, de Kleer I, Arets B, Prakken B, et al. Der p 1-induced
740 CD4(+)FOXP3(+)GATA3(+) T cells have suppressive properties and contribute to the polarization of the
741 TH2-associated response. J Allergy Clin Immunol. 2013;132(6):1440-44.
742 67. Feuerer M, Herrero L, Cipolletta D, Naaz A, Wong J, Nayer A, et al. Lean, but not obese, fat is
743 enriched for a unique population of regulatory T cells that affect metabolic parameters. Nat Med.
744 2009;15(8):930-9.
745 68. Garg G, Muschaweckh A, Moreno H, Vasanthakumar A, Floess S, Lepennetier G, et al. Blimp1
746 Prevents Methylation of Foxp3 and Loss of Regulatory T Cell Identity at Sites of Inflammation. Cell Rep.
747 2019;26(7):1854-68 e5.
748 69. Kusam S, Toney LM, Sato H, Dent AL. Inhibition of Th2 differentiation and GATA-3 expression by
749 BCL-6. J Immunol. 2003;170(5):2435-41.
750 70. Besnard AG, Togbe D, Guillou N, Erard F, Quesniaux V, Ryffel B. IL-33-activated dendritic cells are
751 critical for allergic airway inflammation. Eur J Immunol. 2011;41(6):1675-86.
752 71. Zoltowska AM, Lei Y, Fuchs B, Rask C, Adner M, Nilsson GP. The interleukin-33 receptor ST2 is
753 important for the development of peripheral airway hyperresponsiveness and inflammation in a house
754 dust mite mouse model of asthma. Clin Exp Allergy. 2016;46(3):479-90.
755 72. Vannella KM, Ramalingam TR, Borthwick LA, Barron L, Hart KM, Thompson RW, et al.
756 Combinatorial targeting of TSLP, IL-25, and IL-33 in type 2 cytokine-driven inflammation and fibrosis. Sci
757 Transl Med. 2016;8(337):337ra65.
758 73. Verma M, Liu S, Michalec L, Sripada A, Gorska MM, Alam R. Experimental asthma persists in IL-
759 33 receptor knockout mice because of the emergence of thymic stromal lymphopoietin-driven IL-9(+)
760 and IL-13(+) type 2 innate lymphoid cell subpopulations. J Allergy Clin Immunol. 2018;142(3):793-803 e8.
761 74. Matta BM, Lott JM, Mathews LR, Liu Q, Rosborough BR, Blazar BR, et al. IL-33 is an
762 unconventional Alarmin that stimulates IL-2 secretion by dendritic cells to selectively expand IL-
763 33R/ST2+ regulatory T cells. J Immunol. 2014;193(8):4010-20.

764

765

766 **Figure Legends**

767

768 **Figure 1. Tfr-deficiency results in exacerbated airway inflammation**

769 WT, *Bcl6* $^{fl/fl}$ Foxp3-cre and CD4-cre mice were challenged with 25 μg of HDM extract every
770 other day for 16 days. (a) Schematic of HDM extract-induced airway inflammation model. (b-e)
771 Flow cytometric analysis of CXCR5 and PD-1 on Tfr (gated $CD4^+$ $Foxp3^+$) and Tfh
772 ($CD4^+Foxp3^-$) cells in mediastinal lymph nodes (mLNs). Representative dot plots (b, d) and
773 average percentage (c, e) of Tfr and Tfh cells. (f, g) Flow cytometric analysis of GL7 and Fas on
774 B220 B cells in mLN. Representative dot plot (f) and average percentage (g) of GC B cells. (h)
775 Concentration of HDM specific IgE, IgG1 and total IgE in the serum measured by ELISA. (i-k)
776 Numbers of total cells, eosinophils, neutrophils (i), IL-4-, IL-13- or IL-17-producing $CD4^+$ T
777 cells and eosinophils in the BAL (j) and lung (k). BAL and lung cells were re-stimulated with
778 PMA/ionomycin for 5 hours to measure cytokine production using intracellular staining. Cells
779 for flow cytometric analysis were gated on lymphocyte size and granularity, and the expression
780 of CD4. Data are mean ± SEM of 8-10 mice per group and representative of three independent
781 experiments. A Student's unpaired two-tailed *t* test was used to generate *p* values. **p* < 0.05, ***p*
782 <0.01, ****p* <0.001, *****p*<0.0001

783

784 **Figure 2. Bcl6-deficiency in Treg cells leads to increased $ST2^+$ Treg cell development**

785 Mice were challenged as in Fig. 1. (a, b) Flow cytometric analysis of $ST2^+$ Treg in lung and
786 mLN. (c) Number of $ST2^-$ Treg cells (comparison marked by '*') and $ST2^+$ Treg cells
787 (comparison marked by '†') in lung. (d) ST2 gMFI of $ST2^+$ Treg cells in lung. (e, f) Flow
788 cytometric analysis of $ST2^+$ Tconv cells in lung and mLN. Staining for CXCR5 and ST2 is

shown on cells gated for lymphocyte size and granularity, CD4, and either Foxp3-positive (a-b) or Foxp3-negative (e-f) populations. Representative dot plots (a, e) and average percentages of $ST2^+$ Treg in Treg (left) and in total $CD4^+$ T cells (right) (b) or $ST2^+$ Tconv in $CD4^+$ Tconv (left) and in total $CD4^+$ T cells (right) (f) are shown. Data are mean ± SEM of 8-10 mice per group and representative of three independent experiments. A Student's unpaired two-tailed *t* test was used to generate *p* values. **p* < 0.05, ***p* <0.01, ****p* <0.001, *****p*<0.0001; $^{††}p$ <0.01, $^{†††}p$ <0.001.

Figure 3. Pro-inflammatory transcriptional profile of $ST2^+$ Treg cells in allergic airway inflammation

Treg cells in mLN of HDM challenged WT mice were sorted based on the expression of CD4, Foxp3-YFP and activation markers. (a) TF gene expression was measured using qPCR. (b) Bcl6-expressing Treg cell population was measured using intracellular staining. (c) Th2 cytokine gene expression was measured using qPCR. All gene expression was normalized to *β2m* expression. Student's unpaired two-tailed *t* test was used to generate *p* values. **p* < 0.05, ***p* <0.01, ****p* <0.001, *****p*<0.0001. (d-g) $ST2^+$ Treg and $ST2^-$ Treg cells in lung of HDM challenged WT mice were sorted based on expression of CD4, Foxp3-YFP and ST2. (b-e) Analysis of RNA-seq of sorted $ST2^+$ and $ST2^-$ Treg cells (each from two biological samples) from lung tissues of HDM challenged WT mice. (d) Volcano plot comparing gene expression in $ST2^+$ vs $ST2^-$ Treg cells, (e) Heat maps showing differential expression of genes related to functions (left) and genes aligned with VAT Treg and peripheral Treg cells (pTreg) (right), (f) GSEA of $ST2^+$ vs $ST2^-$ Treg cells with a VAT Treg vs pTreg cells gene list, (g) Ontology analysis of gene enrichment in biological process in $ST2^+$ Treg cells

Figure 4. Bcl6 inhibits and Blimp1 promotes ST2 expression in Treg cells

Splenic Treg cells from WT and *Bcl6*$^{fl/fl}$ Foxp3-cre mice were sorted and stimulated with anti-CD3, anti-CD28 and IL-2 with or without IL-33 (10 ng/ml) for 3 days. Representative dot plots (a) and average percentage (b) of ST2$^+$ Treg cells. (c-d) qPCR analysis of *Il1rl1* and transcription factor genes expression. (e) WT and *Bcl6* $^{fl/fl}$ Foxp3-cre mice were challenged intranasally with 0.5 μg of IL-33 for 3 consecutive days. Average percentage of ST2$^+$ Treg cells in lung. (f-h) Splenic Treg cells from WT and *Prdm1*$^{fl/fl}$ Foxp3-cre mice were sorted and stimulated with anti-CD3, anti-CD28 and IL-2 with or without IL-33 (10ng/ml) for 3 days. Representative dot plots (f) and average percentages (g) of ST2$^+$ Treg cells. (h) qPCR analysis of *Il1rl1*. (i) WT and *Prdm1*$^{fl/fl}$ Foxp3-cre mice were challenged to HDM as in Fig 1. Average percentage of ST2$^+$ Treg cells in lung. (c, d, h) Gene expression was normalized to *β2m* expression. A Student's unpaired two-tailed *t* test was used to generate *p* values. **p* < 0.05, ***p* <0.01, ****p* <0.001, *****p*<0.0001. Data are mean ± SEM of 3-5 mice per group and representative of two independent experiments.

Figure 5. ST2$^+$ Treg cells promote airway inflammation.

ST2$^+$ Treg and Tconv cells were sorted from the lungs of HDM-challenged WT or *Bcl6* $^{fl/fl}$ Foxp3-cre and adoptively transferred to recipient mice. Following transfer, mice were challenged three times with HDM. (a) Schematic adoptive transfer experiment. (b) Number of total BAL cells. Number of total lung cells, neutrophils, eosinophils (c) and total CD4$^+$ T cells (d) in lung. (e) Percentage of donor CD4$^+$ T cells, ST2$^+$ Treg and ST2$^+$ Tconv cells in lung of recipient mice. (f) ST2$^+$ and ST2$^-$ Treg cells in lungs of HDM challenged WT or *Bcl6* $^{fl/fl}$ Foxp3-cre mice were sorted based on the expression of CD4, Foxp3-YFP and ST2. Gene expression was measured

using qPCR and normalized to *β2m* expression. In (b) a student's unpaired two-tailed *t* test was used to compare WT PBS to other groups. In (c-e) One-way ANOVA with a post hoc Tukey test was used to generate *p* values for multiple comparisons. ***p<0.001, ****p<0.0001. Data are mean ± SEM of 6 mice per group pooled from separate analyses. In (f) a Student's unpaired two-tailed *t* test was used to generate *p* values. *p < 0.05, **p <0.01, ***p <0.001, ****p<0.0001

Figure 6. ST2-deficiency compensates for the lack of Bcl6 in Treg cells during allergic airway inflammation

WT, *Bcl6* $^{fl/fl}$ Foxp3-cre, *Il1rl1* $^{-/-}$ and *Il1rl1* $^{-/-}$*Bcl6* $^{fl/fl}$ Foxp3-cre mice were challenged as in Fig 1. (a) Flow cytometric analysis of Tfr, Tfh and GC B cells in mLN. (b) Concentration of HDM specific IgE, IgG1 and total IgE in the serum measured by ELISA. Number of total BAL cells and eosinophils (c), lung cells (d), percentage of IL-13 producing $CD4^+$ T cells (e) and GATA3 expressing Tconv cells (f) in lung tissues. (g) GATA3 expressing Treg cells in lung. Lung cells were re-stimulated with PMA/ionomycin for 5 hours to measure cytokine production using intracellular staining. Cells for flow cytometric analysis were gated on lymphocyte size and granularity, and the expression of CD4. Data are mean ± SEM of 8-10 mice per group and representative of three independent experiments. Student's unpaired two-tailed *t* test was used to generate *p* values. *p < 0.05, **p <0.01, ***p <0.001, ****p<0.0001.

Figure 7. Schematic diagram to describe the roles of Bcl6 on the regulation of IL-33 mediated $ST2^+$ Treg cell development exacerbating allergic airway inflammation.

Figure 1

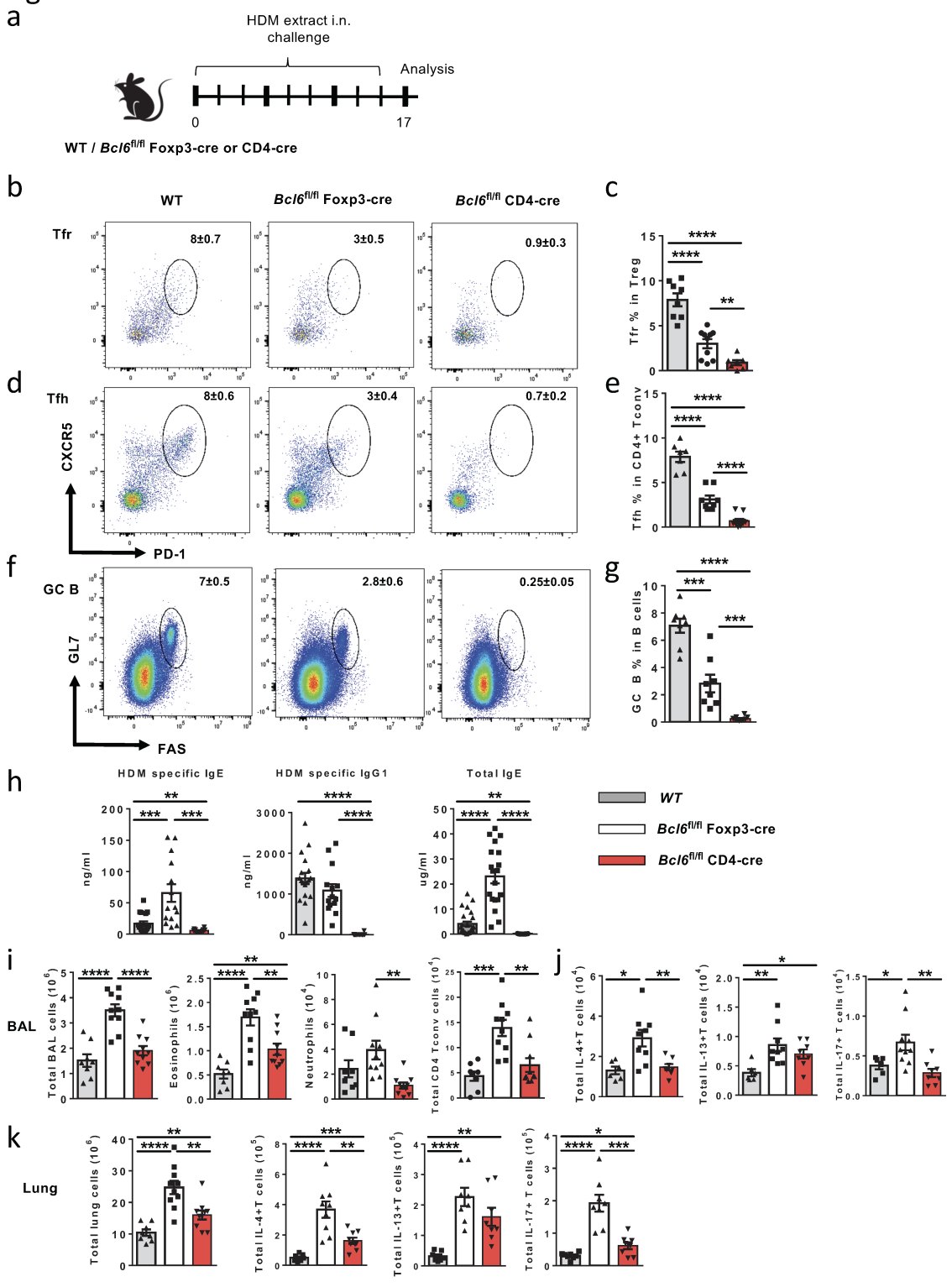
a
HDM extract i.n.
challenge
Analysis
0
17
WT / Bcl6fl/fl Foxp3-cre or CD4-cre
b
WT
Bcl6fl/fl Foxp3-cre
Bcl6fl/fl CD4-cre
Tfr
8±0.7
3±0.5
0.9±0.3
c
Tfr % in Treg
d
Tfh
CXCR5
PD-1
8±0.6
3±0.4
0.7±0.2
e
Tfh % in CD4+ Tconv
f
GC B
GL7
FAS
7±0.5
2.8±0.6
0.25±0.05
g
GC B % in B cells
h
HDM specific IgE
HDM specific IgG1
Total IgE
ng/ml
ug/ml
WT
Bcl6fl/fl Foxp3-cre
Bcl6fl/fl CD4-cre
i
BAL
Total BAL cells (10^6)
Eosinophils (10^6)
Neutrophils (10^4)
Total CD4 Tconv cells (10^4)
j
Total IL-4+T cells (10^4)
Total IL-13+T cells (10^4)
Total IL-17+ T cells (10^4)
k
Lung
Total lung cells (10^6)
Total IL-4+T cells (10^5)
Total IL-13+T cells (10^5)
Total IL-17+ T cells (10^5)

Figure 2

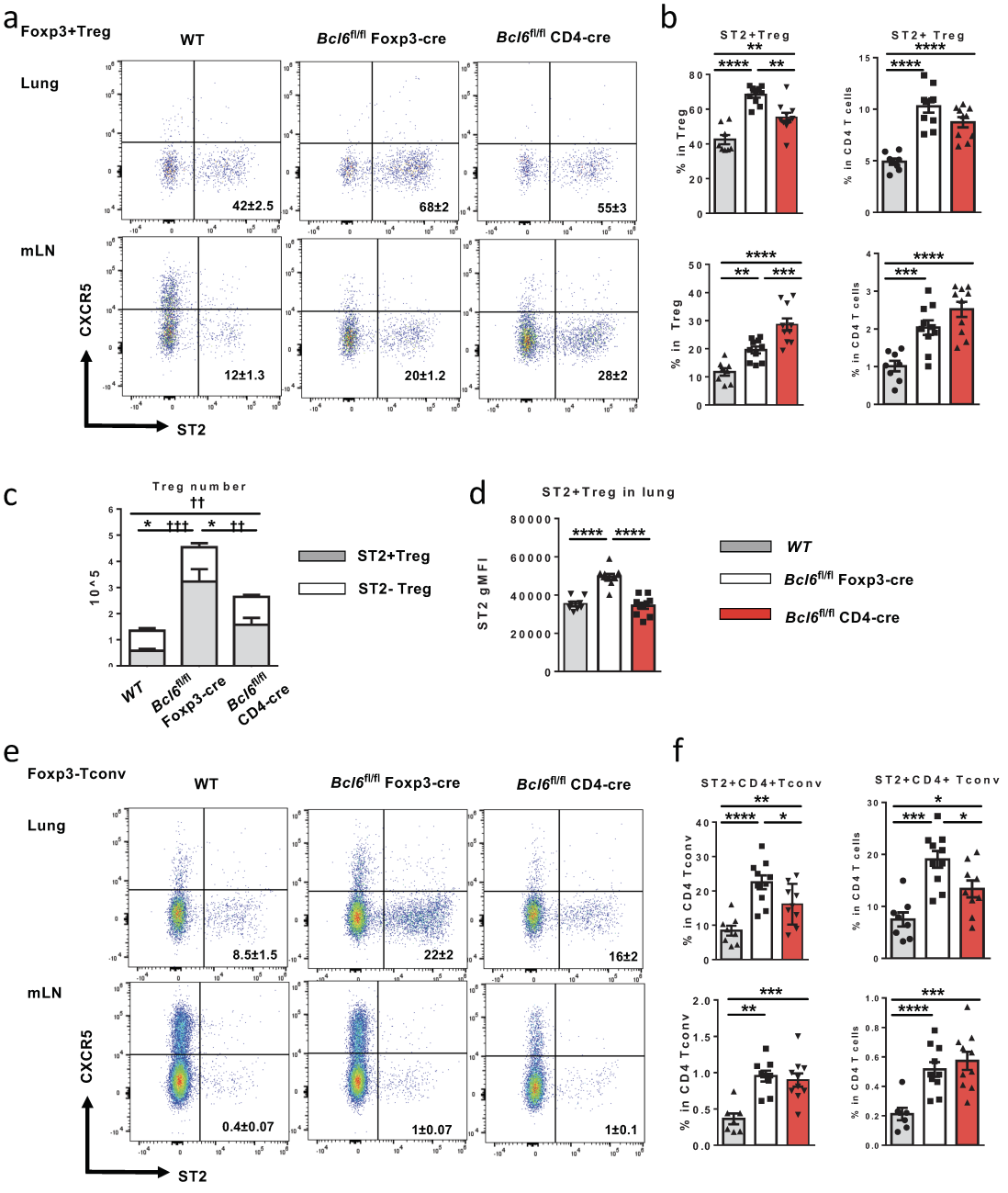
a
Foxp3+Treg
WT
Bcl6fl/fl Foxp3-cre
Bcl6fl/fl CD4-cre
Lung
mLN
CXCR5
ST2
42±2.5
68±2
55±3
12±1.3
20±1.2
28±2
b
ST2+Treg
ST2+ Treg
% in Treg
% in CD4 T cells
c
Treg number
10^5
ST2+Treg
ST2- Treg
WT
Bcl6fl/fl Foxp3-cre
Bcl6fl/fl CD4-cre
d
ST2+Treg in lung
ST2 gMFI
WT
Bcl6fl/fl Foxp3-cre
Bcl6fl/fl CD4-cre
e
Foxp3-Tconv
WT
Bcl6fl/fl Foxp3-cre
Bcl6fl/fl CD4-cre
Lung
mLN
CXCR5
ST2
8.5±1.5
22±2
16±2
0.4±0.07
1±0.07
1±0.1
f
ST2+CD4+Tconv
ST2+CD4+ Tconv
% in CD4 Tconv
% in CD4 T cells

Figure 3

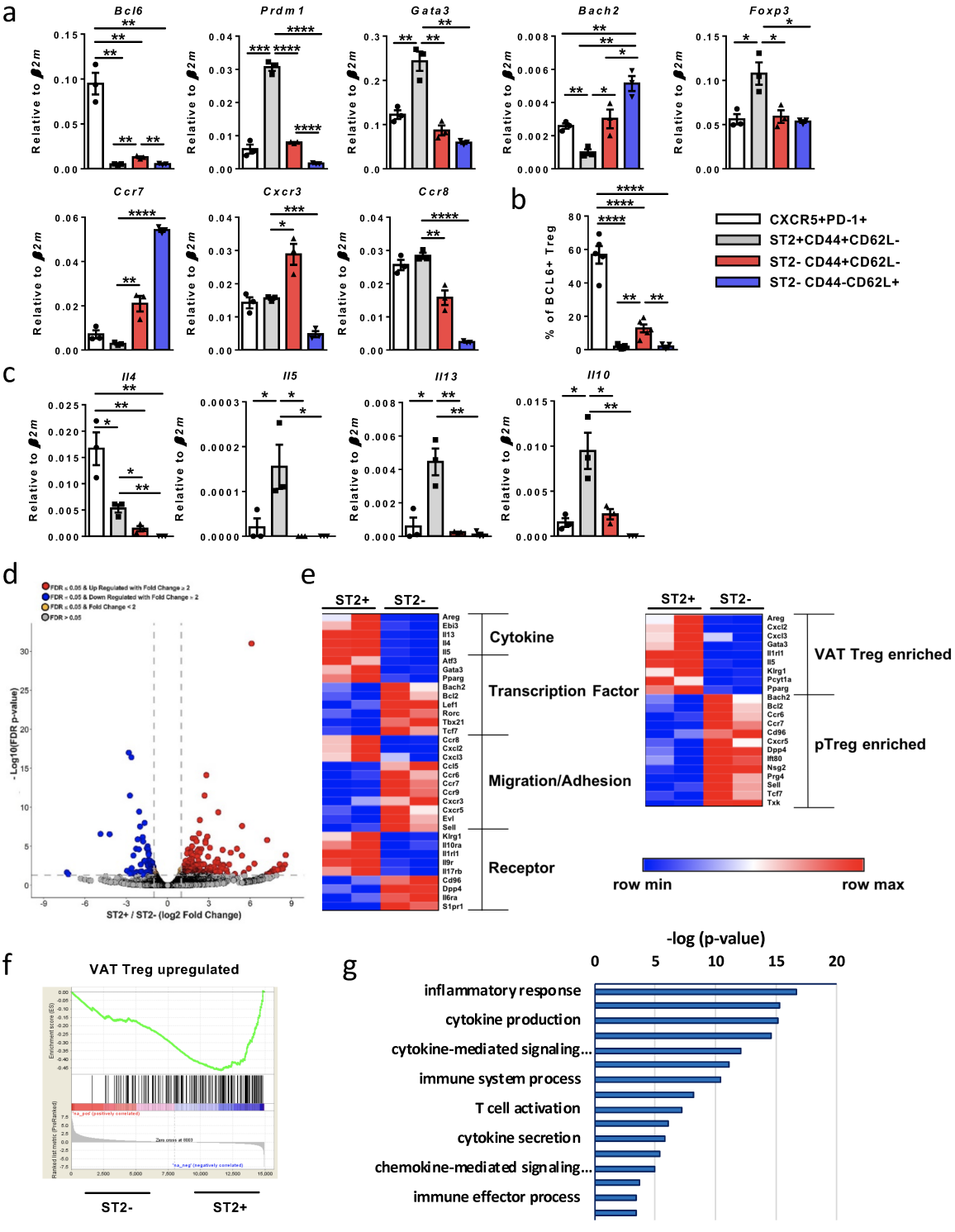
a
Bcl6
Prdm1
Gata3
Bach2
Foxp3
Ccr7
Cxcr3
Ccr8
Relative to β2m
b
% of BCL6+ Treg
CXCR5+PD-1+
ST2+CD44+CD62L-
ST2- CD44+CD62L-
ST2- CD44-CD62L+
c
Il4
Il5
Il13
Il10
d
FDR ≤ 0.05 & Up Regulated with Fold Change ≥ 2
FDR ≤ 0.05 & Down Regulated with Fold Change ≥ 2
FDR ≤ 0.05 & Fold Change < 2
FDR > 0.05
- Log10(FDR p-value)
ST2+ / ST2- (log2 Fold Change)
e
ST2+
ST2-
Areg
Ebi3
Il13
Il4
Il5
Atf3
Gata3
Pparg
Bach2
Bcl2
Lef1
Rorc
Tbx21
Tcf7
Ccr8
Cxcl2
Cxcl3
Ccl5
Ccr6
Ccr7
Ccr9
Cxcr3
Cxcr5
Evl
Sell
Klrg1
Il10ra
Il1r1
Il9r
Il17rb
Cd96
Dpp4
Il6ra
S1pr1
Cytokine
Transcription Factor
Migration/Adhesion
Receptor
Cxcl2
Cxcl3
Gata3
Il1r1
Il5
Klrg1
Pcyt1a
Pparg
Bach2
Bcl2
Ccr6
Ccr7
Cd96
Cxcr5
Dpp4
Ifit80
Nsg2
Prg4
Sell
Tcf7
Txk
VAT Treg enriched
pTreg enriched
row min
row max
f
VAT Treg upregulated
ST2-
ST2+
g
-log (p-value)
inflammatory response
cytokine production
cytokine-mediated signaling...
immune system process
T cell activation
cytokine secretion
chemokine-mediated signaling...
immune effector process

Figure 4

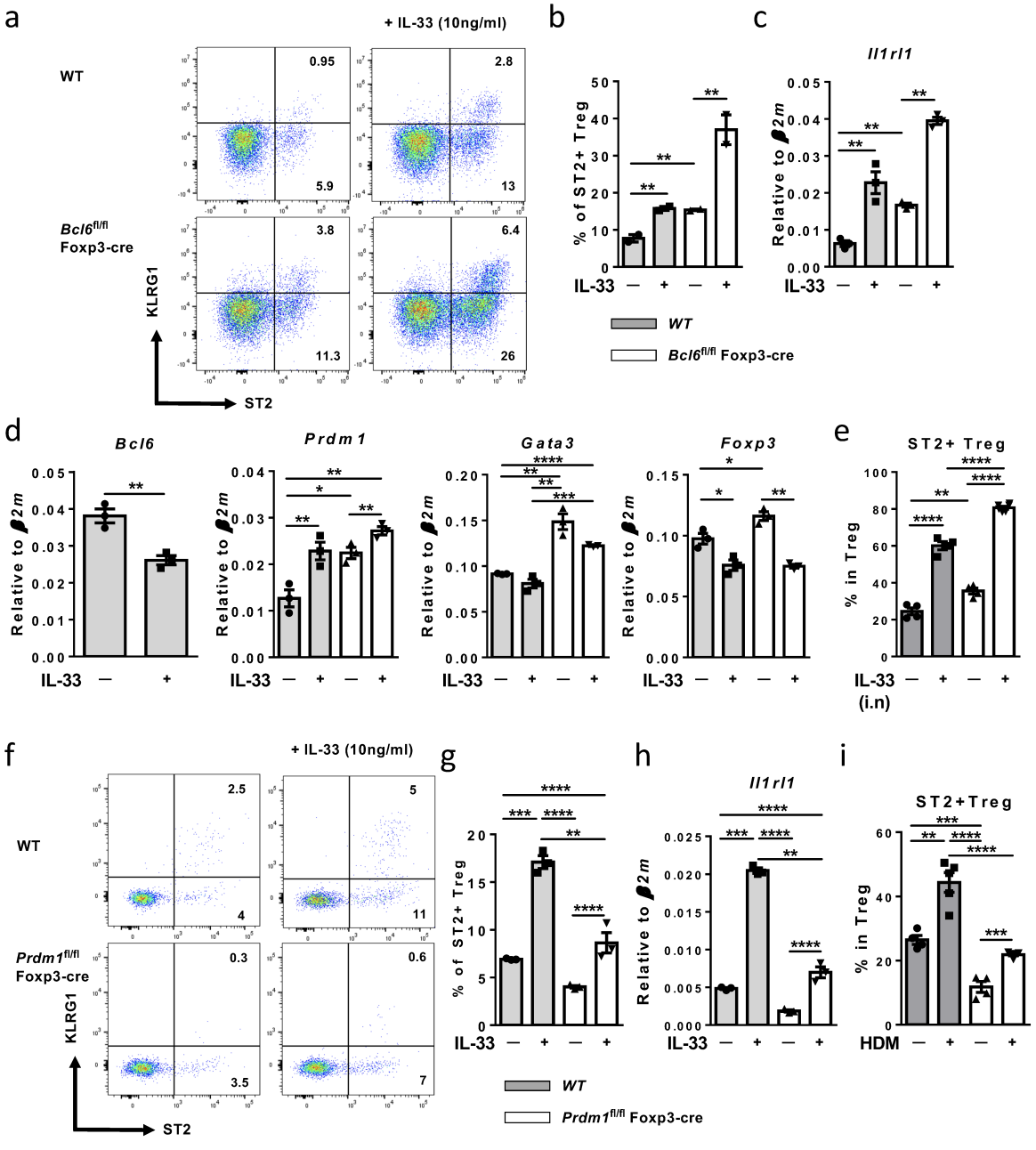
a
+ IL-33 (10ng/ml)
WT
Bcl6fl/fl Foxp3-cre
KLRG1
ST2
0.95
2.8
5.9
13
3.8
6.4
11.3
26
b
% of ST2+ Treg
IL-33
WT
Bcl6fl/fl Foxp3-cre
c
Il1rl1
Relative to β2m
d
Bcl6
Prdm1
Gata3
Foxp3
e
ST2+ Treg
% in Treg
IL-33 (i.n)
f
+ IL-33 (10ng/ml)
Prdm1fl/fl Foxp3-cre
2.5
5
4
11
0.3
0.6
3.5
7
g
h
i
HDM

Figure 5

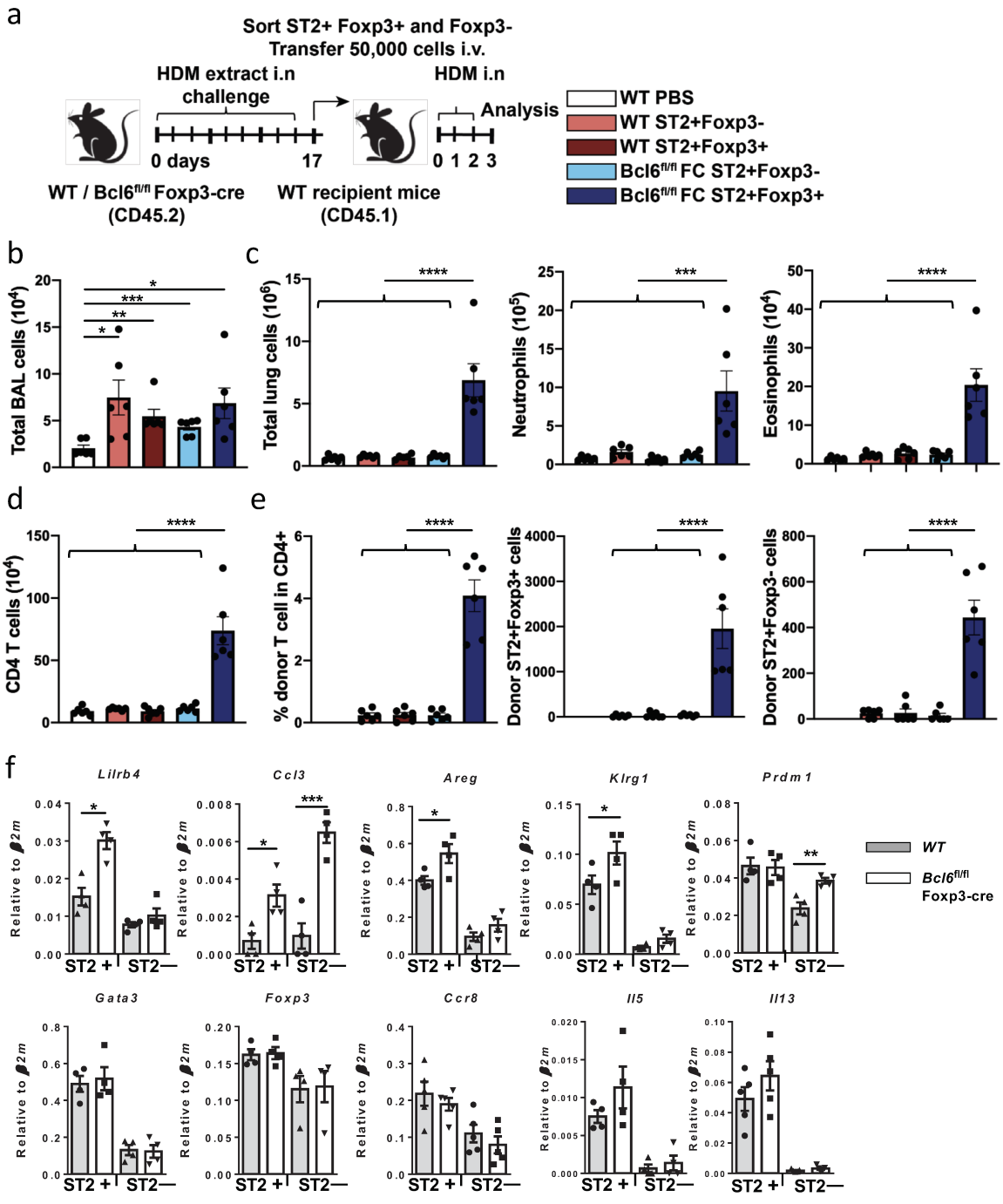
a
Sort ST2+ Foxp3+ and Foxp3-
Transfer 50,000 cells i.v.
HDM extract i.n
challenge
HDM i.n
Analysis
0 days
17
0 1 2 3
WT / Bcl6fl/fl Foxp3-cre
(CD45.2)
WT recipient mice
(CD45.1)
WT PBS
WT ST2+Foxp3-
WT ST2+Foxp3+
Bcl6fl/fl FC ST2+Foxp3-
Bcl6fl/fl FC ST2+Foxp3+
b
Total BAL cells (10⁴)
c
Total lung cells (10⁶)
Neutrophils (10⁵)
Eosinophils (10⁴)
d
CD4 T cells (10⁴)
e
% donor T cell in CD4+
Donor ST2+Foxp3+ cells
Donor ST2+Foxp3- cells
f
Lilrb4
Ccl3
Areg
Klrg1
Prdm1
Gata3
Foxp3
Ccr8
Il5
Il13
Relative to β2m
ST2 +
ST2—
WT
Bcl6fl/fl
Foxp3-cre

Figure 6

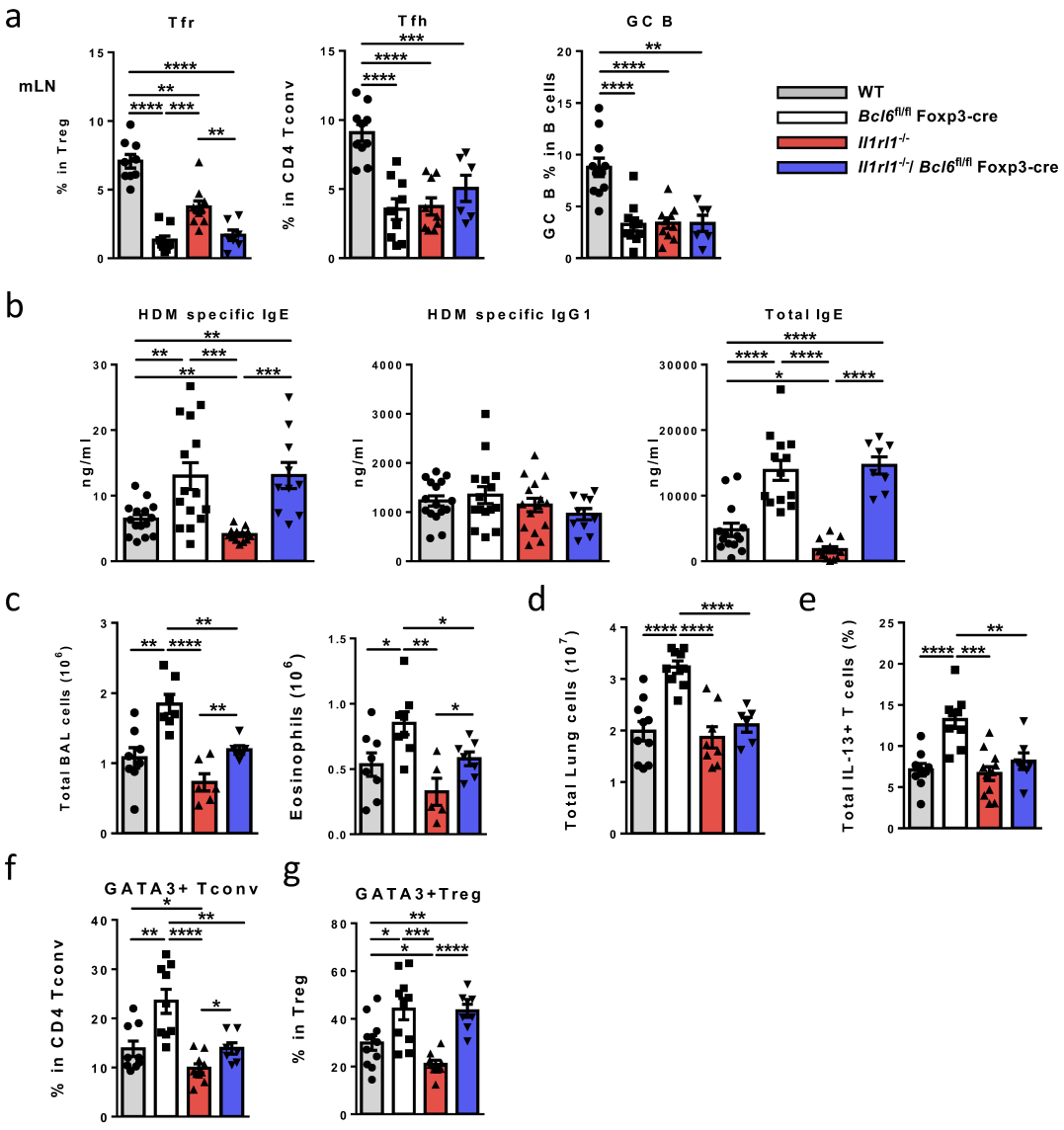
a
Tfr
Tfh
GC B
mLN
% in Treg
% in CD4 Tconv
GC B % in B cells
WT
Bcl6fl/fl Foxp3-cre
Il1rl1-/-
Il1rl1-/- Bcl6fl/fl Foxp3-cre
b
HDM specific IgE
HDM specific IgG1
Total IgE
ng/ml
c
Total BAL cells (10^6)
Eosinophils (10^6)
d
Total Lung cells (10^7)
e
Total IL-13+ T cells (%)
f
GATA3+ Tconv
% in CD4 Tconv
g
GATA3+Treg
% in Treg

Figure 7

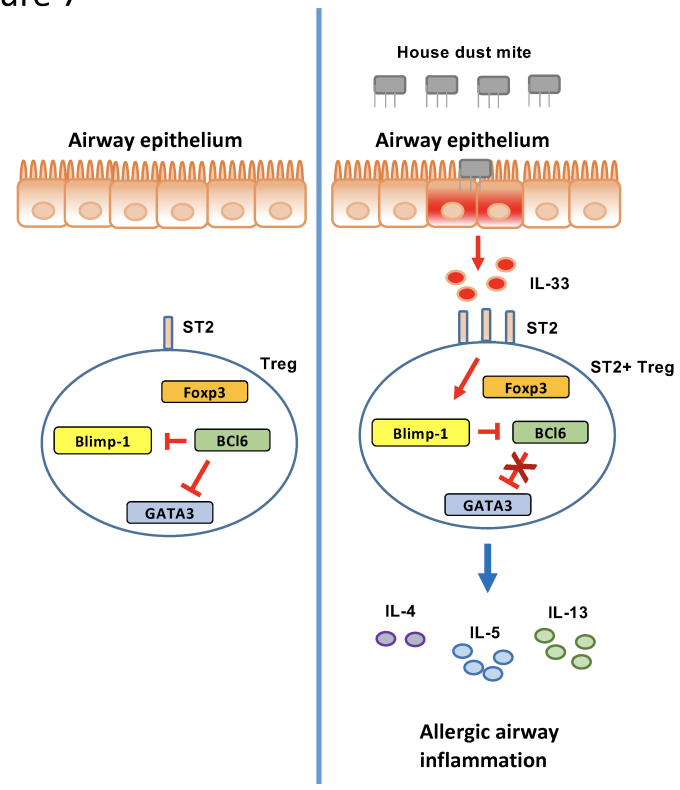
House dust mite
Airway epithelium
Airway epithelium
IL-33
ST2
Treg
Foxp3
Blimp-1
BCl6
GATA3
ST2
ST2+ Treg
Foxp3
Blimp-1
BCl6
GATA3
IL-4
IL-5
IL-13
Allergic airway inflammation

Online Repository Materials

Bcl6 restrains ST2^{+} Treg cell development through negative regulation of Blimp1 in the context of allergic inflammation

Byunghee Koh, PhD [1,2], Benjamin J. Ulrich, PhD [2], Andrew S. Nelson, PhD [1], Gayathri Panangipalli, BS [3], Rakshin Kharwadkar, MS [4], Wenting Wu, PhD [5], Markus M. Xie, PhD [2], Yongyao Fu MS [2], Matthew J. Turner, MD, PhD , Sophie Paczesny, MD, PhD [1,2], Sarath Chandra Janga, PhD [3], Alexander L. Dent, PhD [2], and Mark H. Kaplan, PhD [1,2]

[1]Department of Pediatrics and Herman B Wells Center for Pediatric Research
Indiana University School of Medicine, Indianapolis, IN 46202

[2] Department of Microbiology and Immunology, Indiana University School of Medicine, Indianapolis, IN, 46202

[3] Department of Biohealth Informatics, School of Informatics and Computing, Indiana University-Purdue University, Indianapolis, IN 46202

[4] Department of Biochemistry and Molecular Biology, Indiana University School of Medicine, Indianapolis, IN, 46202

[5] Department of Medical and Molecular Genetics, Indiana University School of Medicine, Indianapolis, IN, 46202

[6] Department of Dermatology, Richard L. Roudebush VA Medical Center, Indianapolis, IN 46202

Corresponding author

Mark H Kaplan, PhD

Indiana University School of Medicine

Department of Microbiology and Immunology

635 Barnhill Dr., Room 420

Indianapolis, IN 46202

United States of America

Ph: +1-317-278-3696

Email: mkaplan2@iu.edu

TABLES

Table E1. Taqman probes for qPCR

Gene	Cat. No.
Areg	Mm00437583_m1
β2m	Mm00437762_m1
Bach2	Mm00464379_m1
Bcl6	Mm00477633_m1
Ccl3	Mm00441259_g1
Ccr7	Mm00432608_m1
Ccr8	Mm00843415_s1
Ctla4	Mm00486849_m1
Cxcr3	Mm00438259_m1
Foxp3	Mm00475165_m1
Gata3	Mm00484683_m1
Il10	Mm00439614_m1
Il13	Mm00434204_m1
Il1rl1	Mm00516117_m1
Il4	Mm00445259_m1
Il5	Mm00439646_m1
Klrg1	Mm00516879_m1
Lilrb4	Mm01614371_m1
Prdm1	Mm00476128_m1
Tnfrsf18	Mm00437136_m1

Table E2. Fluorescent antibodies for flow cytometric analysis

Antigen/Name	Clone	Fluorochrome	Company	Cat. No.
B220	RA3-6B2	PerCP-Cy5.5	BioLegend	103236
BCL-6	K112-91	BV421	BD Biosciences	563363
CD11b	M1/70	PerCP-Cy5.5	eBioscience	45-0112-82
CD11c	N418	PE-Cy7	eBioscience	25-0114-82
CD4	GK1.5	PerCP-Cy5.5	BioLegend	100434
		APC-Cy7	BioLegend	552051
CD44	IM7	BV510	BD Biosciences	563114
CD62L	MEL-14	APC	BD Biosciences	553152
CXCR5	L138D7	PE-Cy7	BioLegend	145516
F4/80	BM8	FITC	BioLegend	123108
FAS (CD95)	SA367H8	PE	BioLegend	152608
Foxp3	MF23	FITC	BD Biosciences	560403
GATA3	L50-823	AF647	BD Biosciences	560068
GL7	GL7	APC	BioLegend	144617
IFN-γ	XMG 1.2	PerCP-Cy5.5	eBioscience	45-7311-82
IL-10	JES5-16E3	FITC	BioLegend	505006
IL-13	eBio13A	PE	eBioscience	12-7133-82
IL-17A	eBio17B7	PE-Cy7	eBioscience	25-7177-82
IL-4	11B11	AF647	BioLegend	504110
KLRG1	2F1	BV510	BD Biosciences	740156
		APC	BD Biosciences	561620
Ly6G	1A8	APC	BioLegend	127613
PD-1	29F.1A12	PerCP-Cy5.5	BioLegend	135208
SiglecF	E50-2440	PE	BD Biosciences	552126
ST2	U29-93	PE	BD Biosciences	566309
Fixable Viability dye		eFluor 780	eBioscience	65-0865-14

Table E3. Sequence of ChIP primers

Mouse		
Primers	Forward (5'-3')	Reverse (5'-3')
Il1rl1 enhancer	GCCAACCACAACAGCAGATGGGGAAA	ACTGAGATCCTGCCCTGGCTTCCCT
Il1rl1 promoter	TGGCCTCCTTGGAAAGGCTTGGT	AGTGCAGGAGGGGCATGGAGATGA
Prdm1 intron	TGCTTTCTCGGTTTCAGTTGA	GAGTGAGCTGCTTTGGAAGG
Prdm1 promoter	CCAGTAGGCCTTTCATGGCT	TGCTCAGGTTGAGAAAGCAGT

FIGURE LEGENDS

Figure E1. Tfr-deficiency results in exacerbated airway inflammation

Mice were sensitized and challenged to HDM as in Figure 1. (a) Representative dot plot (left) and average percentage (right) of $Foxp3^+$ Treg cells in $CD4^+$ T cells in mLN. Percentage of IL-4, IL-13 or IL-17 producing $CD4^+$ T cells in BAL (b) and lung (c). (d) Number of IL-10 producing $CD4^+$ T cells in BAL and lung. (e) Representative dot plots of IL-4 or IL-13 producing $CD4^+$ T cells. Data are mean ± SEM of 8-10 mice per group and representative of three independent experiments. A Student's unpaired two-tailed *t* test was used to generate *p* values. $^{**}p < 0.01$, $^{***}p < 0.001$, $^{****}p < 0.0001$

Figure E2. Bcl6-deficiency in Treg cells leads to increased $ST2^+$ Treg cell development

Mice were sensitized and challenged to HDM as in Figure 1 (a-c, e-h). (a) Average percentage of GATA3 positive cells in $ST2^+$ or $ST2^-$ Treg cells in lung and mLN of WT mice. (b, c) Activation status, $CD44^{high}$ and $CD62L^{low}$, of Treg cells in mLN and lung. Representative dot plots (b) and average percentage (c) of activated Treg cells. (d) Percentages $ST2^+$ Treg and $ST2^+$ Tconv cells in lung or mLN of naïve WT and $Bcl6^{fl/fl}$ Foxp3-Cre mice. Representative dot plots (e) and average percentage (f) of BCL6 expressing Treg cells in $ST2^+$ or $ST2^-$ Treg cells in lung and mLN of WT mice. (g) $ST2^+$ Treg and $ST2^+$ Tconv cells in mesLN. (h) The percentage of Helios-positive Treg cells in lung and mLN. (a-h) Data are mean ± SEM of 4-6 mice per group and representative of two independent experiments. A Student's unpaired two-tailed *t* test was used to generate *p* values. $^{**}p < 0.01$, $^{***}p < 0.001$, $^{****}p < 0.0001$.

Figure E3. $ST2^+Foxp3^+$ Treg cells are present in multiple strains of mice.

Mice were sensitized and challenged to HDM as in Figure 1. Flow cytometric analysis of $ST2^+$ Tregs and $ST2^+$ Tconv cells in the lungs (a) and mLNs (b) of naïve and HDM challenged BALB/cJ and C57BL/6 mice. (c) Increase of cellularity between naïve and HDM challenged mice represented as fold change for each strain tested. A Student's unpaired two-tailed *t* test was used to generate *p* values. $^{**}p < 0.01$.

Figure E4. Pro-inflammatory transcriptional profile of $ST2^+$ Treg cells in allergic airway inflammation

(a) Representative dot plot (left) and percentage (right) of intracellular staining of Th2 cytokines in $ST2^+$ or $ST2^-$ Treg cells. (b-d) $ST2^+$ and $ST2^-$ $Foxp3/YFP^+$ Treg cells were sorted from the lungs of HDM challenged WT mice. Gene expression was measured using qPCR and normalized to *β2m* expression. A Student's unpaired two-tailed *t* test was used to generate *p* values. $^{*}p < 0.05$, $^{**}p < 0.01$, $^{***}p < 0.001$, $^{****}p < 0.0001$.

Figure E5. Bcl6 inhibits and Blimp1 promotes ST2 expression in Treg cells

(a, b) Naïve $CD4^+$ T cells were isolated from spleen of WT and $Bcl6^{fl/fl}$ Foxp3-cre mice and stimulated with anti-CD3, anti-CD28, IL-2 and TGF-β with or without IL-33 (1 or10 ng/ml) for 3 days. qPCR analysis of *Il1rl1* (a) and Bcl6 expression (b). All gene expression was normalized to *β2m* expression. (c) WT mice were challenged with 0.5 μg IL-33 intranasally for 3 consecutive days. $ST2^+$ or $ST2^-$ Treg cells were sorted from lung based on CD4, Foxp3-YFP and ST2 expression. Transcription factor gene expression in $ST2^+$ or $ST2^-$ Treg cells measured using qPCR and normalized to *β2m* expression. (d) Splenic Treg cells from $Il1rl1^{-/-}$ and $Il1rl1^{-/-}Bcl6^{fl/fl}$ Foxp3-cre mice were sorted and stimulated with anti-CD3, anti-CD28 and IL-2 with or without

IL-33 (10 ng/ml) for 3 days. *Il13, Il4* and *Gata3* expression was measured using qPCR. (e, f) WT splenic Treg cells were sorted and stimulated with anti-CD3, anti-CD28, IL-2 with or without IL-33 (10 ng/ml) for 3 days. On day 3, cells were harvested for ChIP analysis for H3K27ac at the *Il1rl1* (e) and *Prdm1* (f) gene loci. (g, h) Splenic Treg cells from WT C57BL/6 and BALB/cJ mice were sorted and stimulated with anti-CD3, anti-CD28 and IL-2 with or without IL-33 (10 ng/ml) for 3 days. Representative dot plots (g) and average percentage (h) of $ST2^+$ Treg cells. (i-k) WT and $Prdm1^{fl/fl}$ Foxp3-cre mice were sensitized and challenged to HDM as in Fig 1. (i) Average percentages of $BCL6^+$ Treg cells in lung. Representative dot plots (j) and average percentage (k) of Tfr cells in mLN. Data are mean ± SEM of 3-5 mice per group and representative of two independent experiments. A Student's unpaired two-tailed *t* test was used to generate *p* values. **p* < 0.05, ***p* <0.01, *****p*<0.0001.

Figure E6. ST2-deficiency compensates for the lack of Bcl6 in Treg cells during allergic airway inflammation

(a) Flow cytometric analysis of $ST2^+$ Treg and Tconv cells in lung and mLN. (b) Flow cytometric analysis of ST2 and KLRG1 expression and (c) total KLRG1 expressing Treg cells in lung. Data are mean ± SEM of 8-10 mice per group and representative of three independent experiments. A Student's unpaired two-tailed *t* test was used to generate *p* values. **p* < 0.05, ***p* <0.01, ****p* <0.001, *****p*<0.0001.

Figure E1

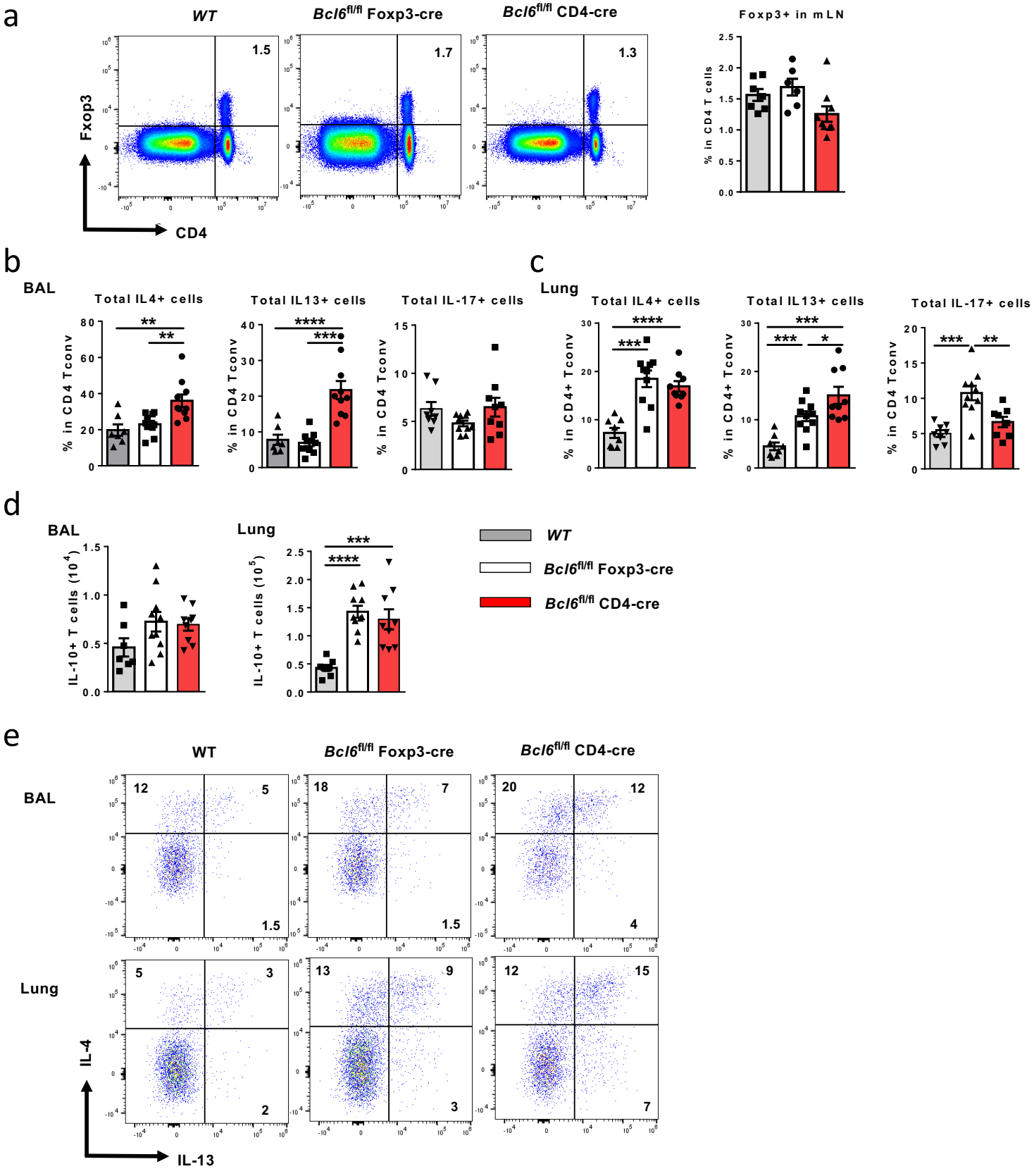
a
WT
Bcl6fl/fl Foxp3-cre
Bcl6fl/fl CD4-cre
Fxop3
CD4
1.5
1.7
1.3
Foxp3+ in mLN
% in CD4 T cells
b
BAL
Total IL4+ cells
Total IL13+ cells
Total IL-17+ cells
% in CD4 Tconv
c
Lung
Total IL4+ cells
Total IL13+ cells
Total IL-17+ cells
% in CD4+ Tconv
d
BAL
Lung
IL-10+ T cells (10^4)
IL-10+ T cells (10^5)
WT
Bcl6fl/fl Foxp3-cre
Bcl6fl/fl CD4-cre
e
WT
Bcl6fl/fl Foxp3-cre
Bcl6fl/fl CD4-cre
BAL
Lung
IL-4
IL-13
12
5
1.5
18
7
1.5
20
12
4
5
3
2
13
9
3
12
15
7

Figure E2

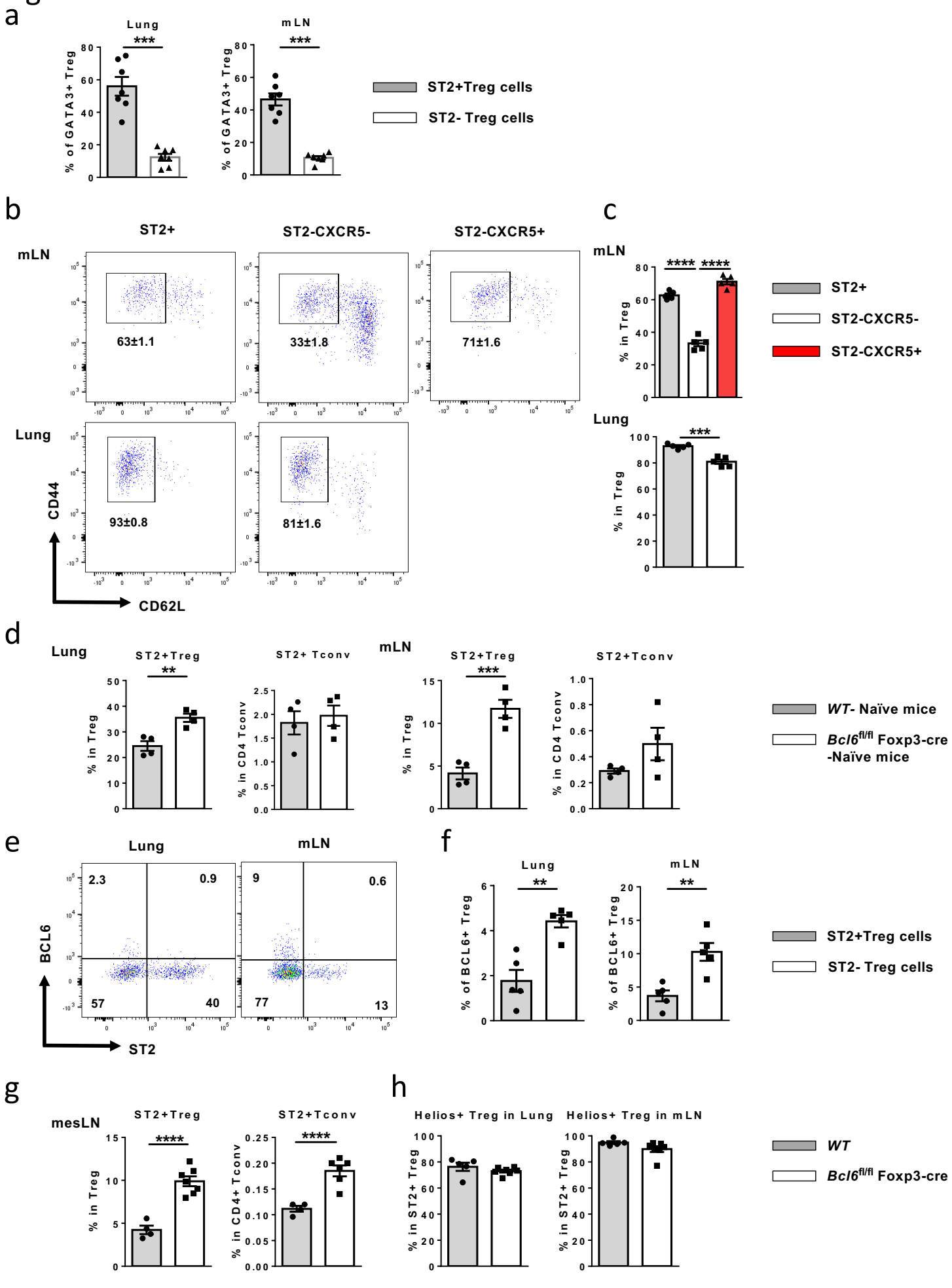
a
Lung
mLN
% of GATA3+ Treg
***
ST2+Treg cells
ST2- Treg cells
b
ST2+
ST2-CXCR5-
ST2-CXCR5+
mLN
63±1.1
33±1.8
71±1.6
Lung
93±0.8
81±1.6
CD44
CD62L
c
mLN
% in Treg
****
ST2+
ST2-CXCR5-
ST2-CXCR5+
Lung
***
d
Lung
ST2+Treg
ST2+ Tconv
% in Treg
% in CD4 Tconv
**
mLN
ST2+Treg
ST2+Tconv
***
WT- Naïve mice
Bcl6fl/fl Foxp3-cre -Naïve mice
e
Lung
mLN
BCL6
ST2
2.3
0.9
57
40
9
0.6
77
13
f
Lung
mLN
% of BCL6+ Treg
**
ST2+Treg cells
ST2- Treg cells
g
mesLN
ST2+Treg
ST2+Tconv
% in Treg
% in CD4+ Tconv
****
h
Helios+ Treg in Lung
Helios+ Treg in mLN
% in ST2+ Treg
WT
Bcl6fl/fl Foxp3-cre

Figure E3

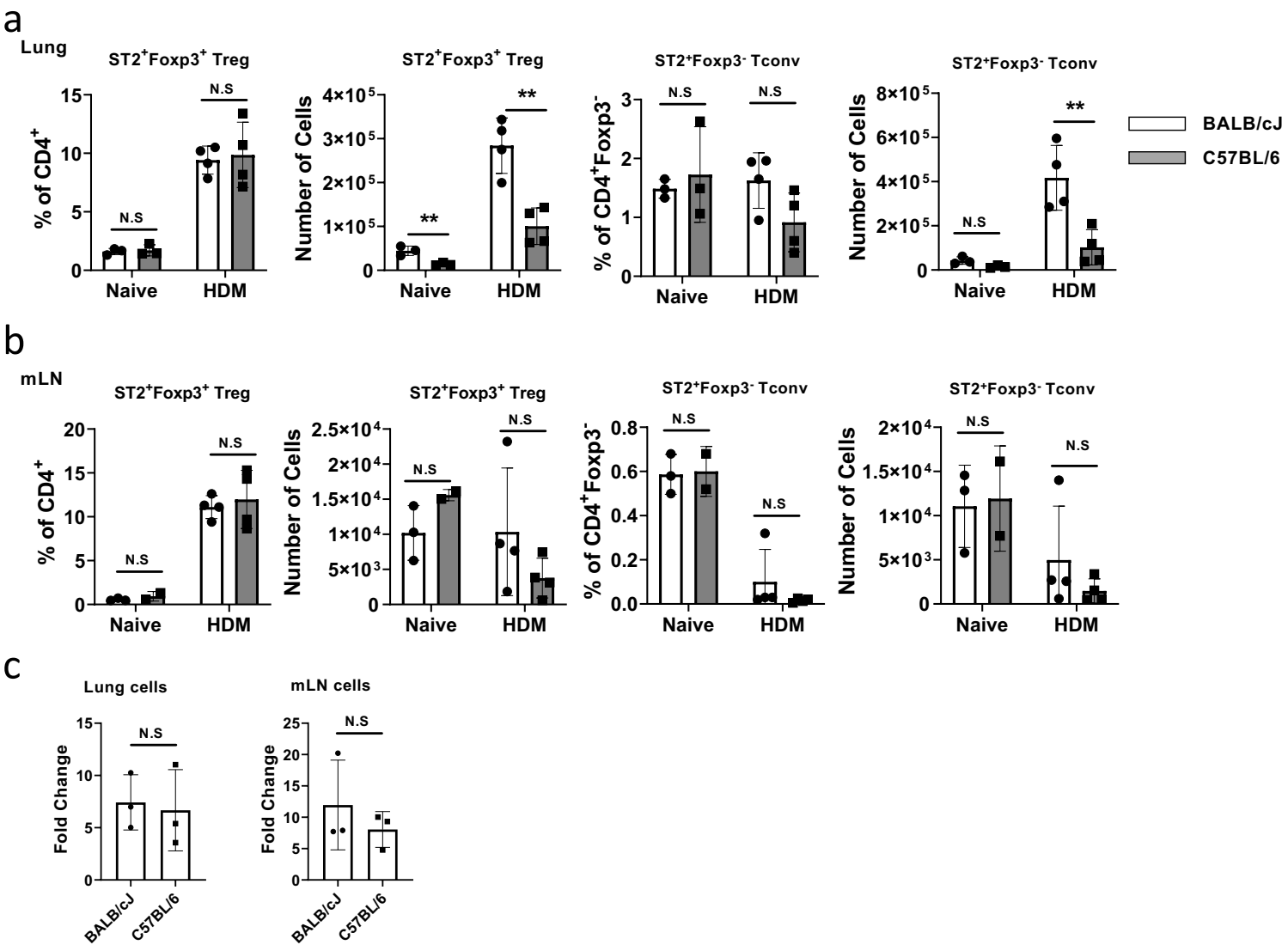
a
Lung
ST2+Foxp3+ Treg
% of CD4+
Number of Cells
ST2+Foxp3- Tconv
% of CD4+Foxp3-
N.S
**
Naive
HDM
BALB/cJ
C57BL/6
b
mLN
c
Lung cells
mLN cells
Fold Change

Figure E4

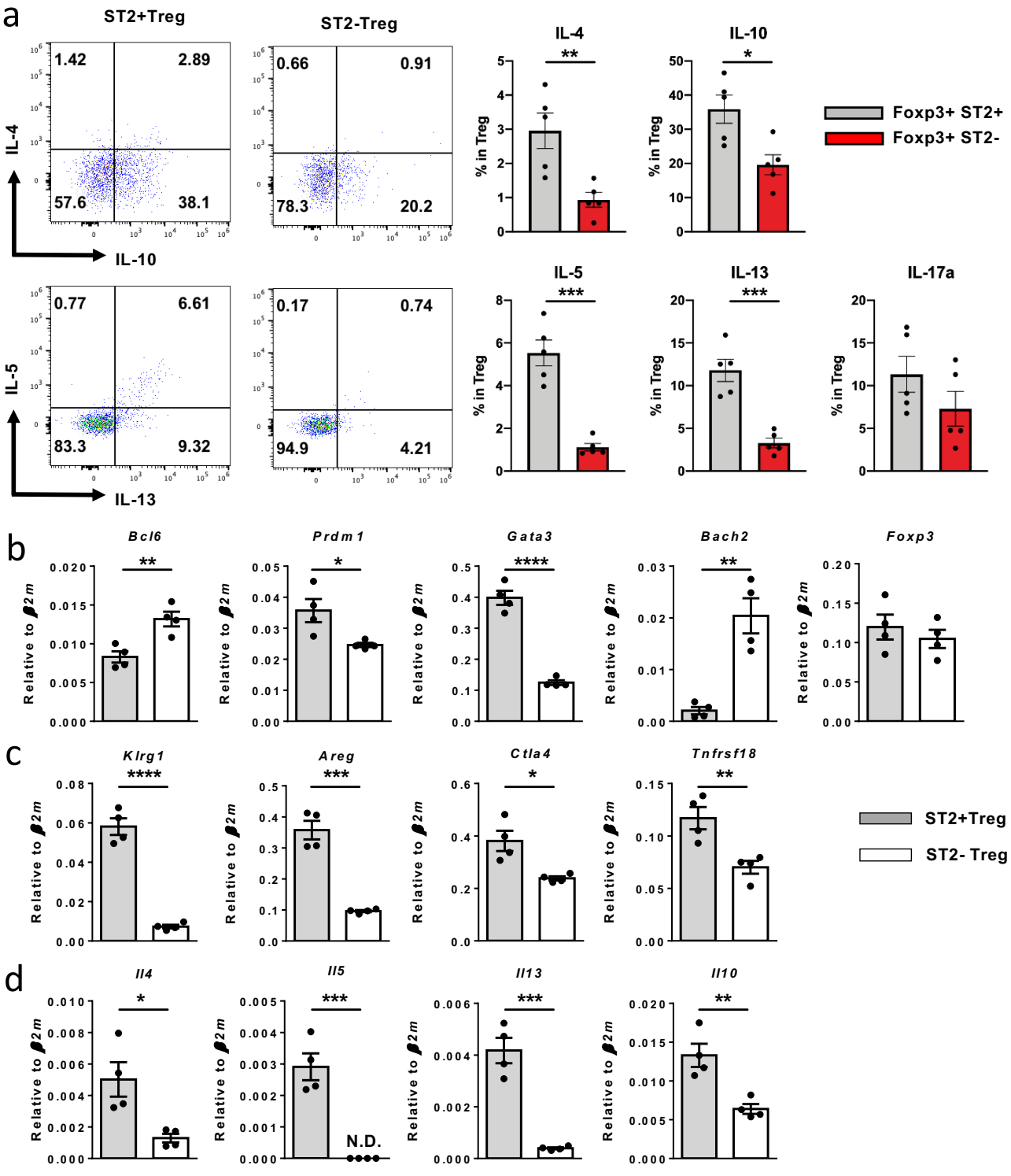
a
ST2+Treg
ST2-Treg
1.42
2.89
57.6
38.1
0.66
0.91
78.3
20.2
IL-4
IL-10
IL-4
IL-10
% in Treg
Foxp3+ ST2+
Foxp3+ ST2-
0.77
6.61
83.3
9.32
0.17
0.74
94.9
4.21
IL-5
IL-13
IL-5
IL-13
IL-17a
b
Bcl6
Prdm1
Gata3
Bach2
Foxp3
Relative to β2m
c
Klrg1
Areg
Ctla4
Tnfrsf18
ST2+Treg
ST2- Treg
d
Il4
Il5
Il13
Il10
N.D.

Figure E5

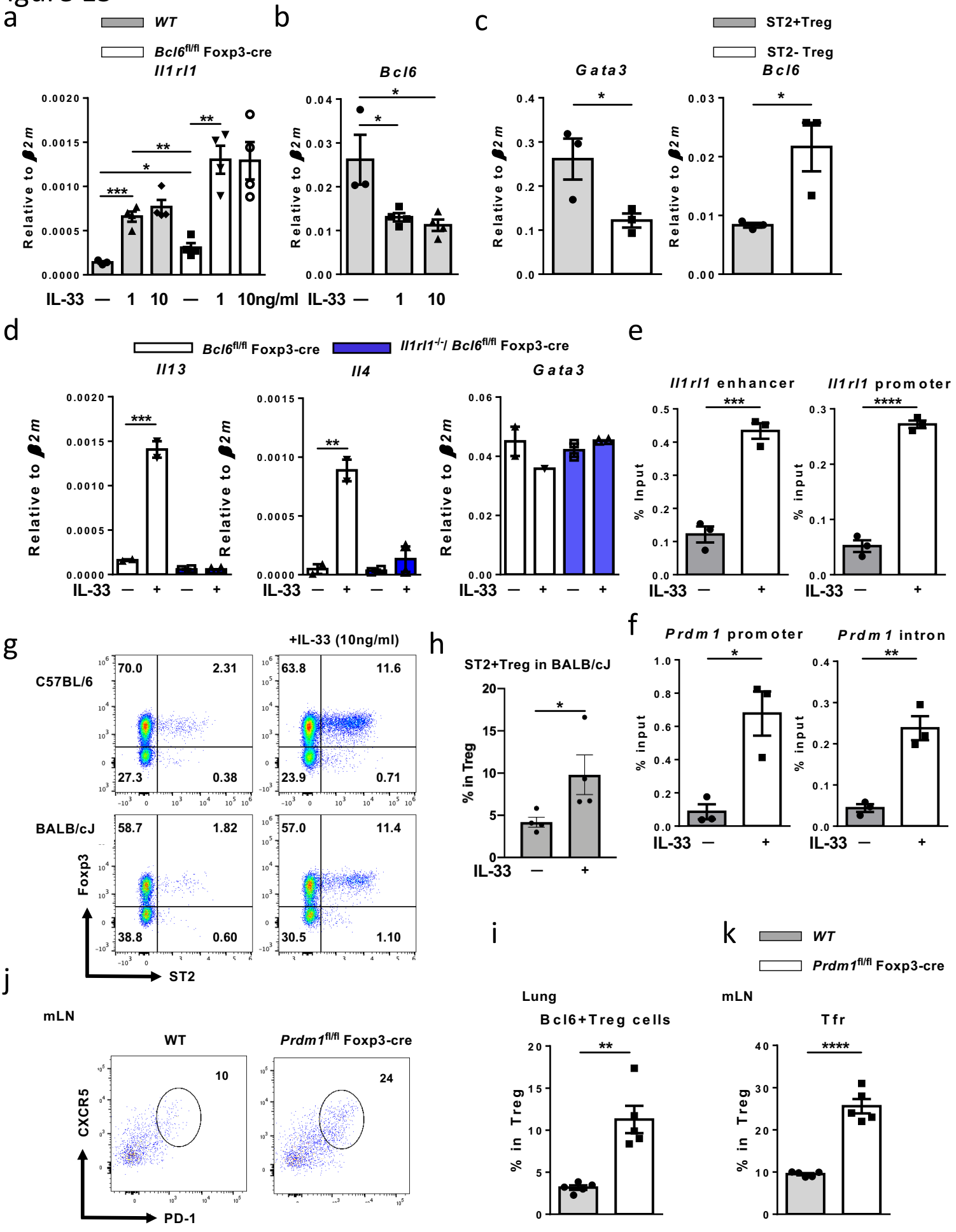
a
WT
Bcl6fl/fl Foxp3-cre
Il1rl1
Relative to β2m
IL-33 — 1 10 — 1 10ng/ml
b
Bcl6
Relative to β2m
IL-33 — 1 10
c
ST2+Treg
ST2- Treg
Gata3
Bcl6
Relative to β2m
d
Bcl6fl/fl Foxp3-cre
Il1rl1-/-/ Bcl6fl/fl Foxp3-cre
Il13
Il4
Gata3
Relative to β2m
IL-33 — + — +
e
Il1rl1 enhancer
Il1rl1 promoter
% input
IL-33 — +
f
Prdm1 promoter
Prdm1 intron
% input
IL-33 — +
g
+IL-33 (10ng/ml)
C57BL/6
70.0
2.31
27.3
0.38
63.8
11.6
23.9
0.71
BALB/cJ
58.7
1.82
38.8
0.60
57.0
11.4
30.5
1.10
Foxp3
ST2
h
ST2+Treg in BALB/cJ
% in Treg
IL-33 — +
i
Lung
Bcl6+Treg cells
% in Treg
k
WT
Prdm1fl/fl Foxp3-cre
mLN
Tfr
% in Treg
j
mLN
WT
Prdm1fl/fl Foxp3-cre
10
24
CXCR5
PD-1

Figure E6

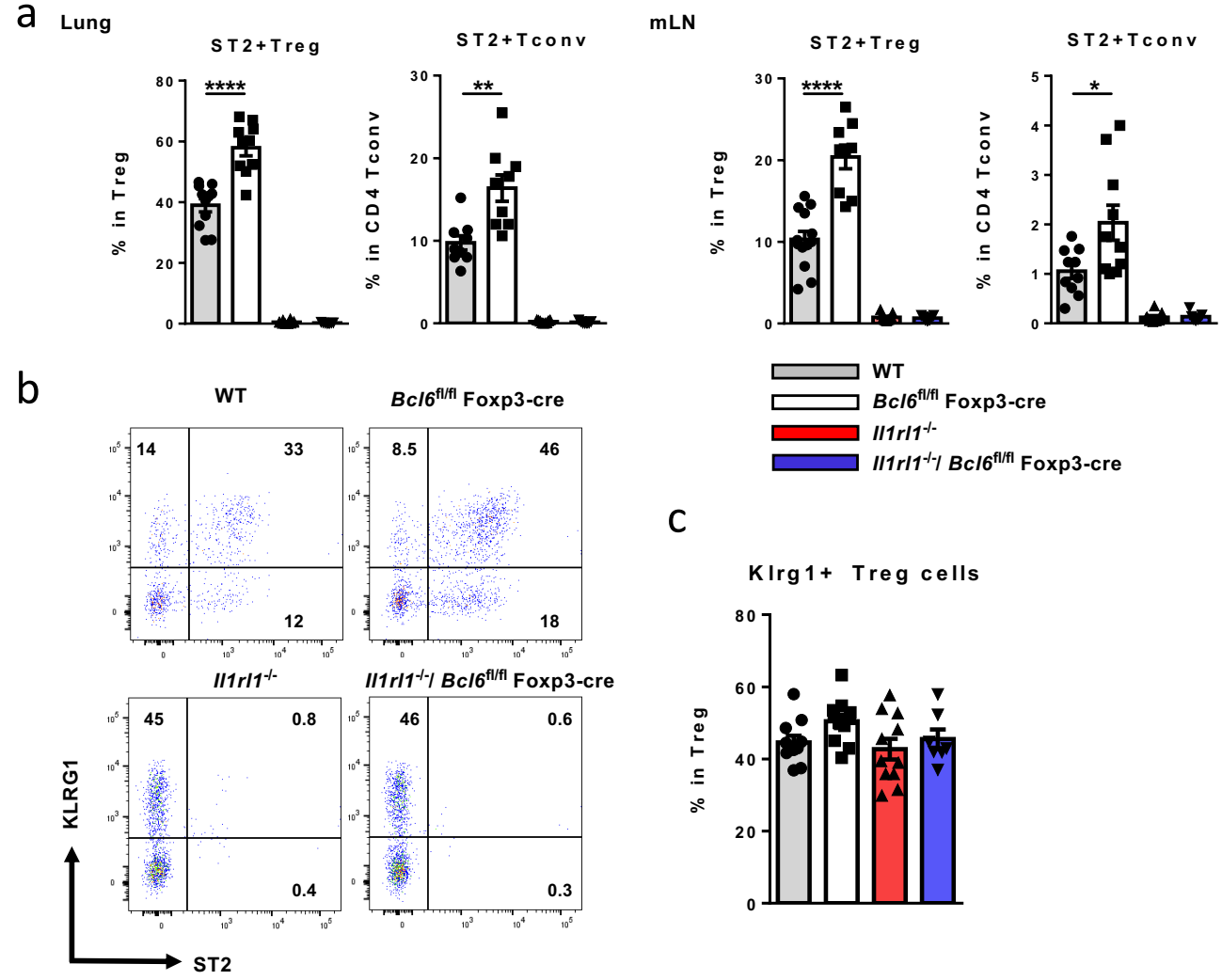
a
Lung
ST2+Treg
ST2+Tconv
% in Treg
% in CD4 Tconv
****
**
mLN
ST2+Treg
ST2+Tconv
% in Treg
% in CD4 Tconv
****
*
b
WT
Bcl6fl/fl Foxp3-cre
Il1rl1-/-
Il1rl1-/- Bcl6fl/fl Foxp3-cre
14
33
12
8.5
46
18
45
0.8
0.4
46
0.6
0.3
KLRG1
ST2
WT
Bcl6fl/fl Foxp3-cre
Il1rl1-/-
Il1rl1-/- Bcl6fl/fl Foxp3-cre
c
Klrg1+ Treg cells
% in Treg